7-30-2013 12:00 AM

Traumatic Injury in vitro Elicits JNK-mediated Human Astrocyte Retraction, but Spares Cerebrovascular Endothelial Cells

Claudia Augustine, *The University of Western Ontario*

Supervisor: Dr. Douglas D. Fraser, *The University of Western Ontario*

A thesis submitted in partial fulfillment of the requirements for the Master of Science degree in Physiology

Traumatic Injury *in vitro* Elicits JNK-mediated Human Astrocyte Retraction, but Spares Cerebrovascular Endothelial Cells

(Thesis format: Monograph)

by

Claudia Augustine

Graduate Program in Physiology

A thesis submitted in partial fulfillment
of the requirements for the degree of
Master of Science

The School of Graduate and Postdoctoral Studies
The University of Western Ontario
London, Ontario, Canada

Abstract

The pathophysiology of a traumatic brain injury (TBI) involves the dysfunction of the blood-brain barrier (BBB). The lumen of the BBB is lined with cerebrovascular endothelial cells (CVEC) that are ensheathed with perivascular astrocyte endfeet. We investigated the cellular response of human-astrocytes and human-CVEC following trauma *in vitro.* Astrocytes and CVEC were subjected to a concussive injury (CI; mechanical stretch), then assessed for markers of injury (monolayer retraction) and activation (mitogen-activated protein kinases (MAPK) phosphorylation).

CI induces astrocyte monolayer retraction and activation, with predominant phosphorylation of JNK1/2 MAPK. Interfering with JNK1/2 activation (selective JNK inhibitors) reduces trauma-induced astrocyte retraction. On the contrary, CI does not induce CVEC retraction, however up-regulates CVEC pro-adhesive phenotype resulting in increased polymorphonuclear leukocyte (PMN) adhesion.

These findings indicate that CI elicits differential BBB cell responses: JNK-mediated astrocyte retraction and CVEC-dependent increase in leukocyte recruitment, the phenomena that may contribute to overall BBB dysfunction following TBI.

Keywords

Traumatic brain injury, concussion, blood-brain barrier, cerebrovascular endothelial cells, astrocytes, astrocyte endfeet, cellular retraction, polymorphonuclear leukocytes, MAP kinases, leukocyte-endothelial cell adhesion

Co-Authorship Statement

Dr. Gediminas Cepinskas and Dr. Douglas Fraser provided valuable guidance in designing the experimental approach and interpreting the data collected in this study. The human immortalized cerebrovascular endothelial cells, hCMEC/D3, employed in our experimentations were generously provided from Dr. Pierre Couraud (ISERM, France). Figures and texts were generated by C Augustine, and then reviewed by D Fraser and G Cepinskas. A portion of this manuscript will be submitted for peer-reviewed publication.

Acknowledgments

I would like to give my sincere thanks to my two wonderful supervisors, Dr. Fraser and Dr. Cepinskas, for all the support and guidance they have provided me as I completed my graduate degree. I would like to thank my advisory committee, Dr. Qingping Feng and Dr. Arthur Brown, for their advisements regarding my project. Thank you to the members of the Fraser/Cepinskas lab for the help they willingly provide for me daily. I would like to give a special thanks to Dr. Jamie Seabrook of the Children's Health Research Institute for providing an independent statistical review of my data analyses. Lastly, I would like to thank Andrew Arifin for providing assistance in generating supplemental graphics/figures found in Chapter 1 (background) of my thesis report.

Table of Contents

Page

List of Figures

List of Abbreviations

ANG1	Angiopoietin 1
ANOVA	Analysis of Variance
AQP4	Aquaporin 4
ATP	Adenosine Triphosphate
BBB	Blood-brain barrier
bFGF	basic Fibroblast Growth Factor
CBF	Cerebral Blood Flow
CFDA	5,6-carboxyfluoroscein diacetate
CM	Cytomix
CNS	Central Nervous System
COX	Cyclooxygenase
CPM	Count Per Minute
CVEC	Cerebrovascular Endothelial Cells
DBS	Diffuse Brain Swelling
EDTA	Ethylenediaminetetraacetic acid
EET	Epoxyeicosatrienoic acid
ELISA	Enzyme-linked Immunosorbent Assay
ERK	Extracellular Signal-regulated Kinase

EnGS	Endothelial Cell Growth Supplement
GAPDH	Glyceraldehyde-3-phosphate Dehydrogenase
GDNF	Glial-derived Neurotrophic Factor
HA	Human Astrocytes
HRP	Horseradish Peroxidase
hCMEC/D3	Human Immortalized Cerebral Microvascular Endothelial Cell Line
ICAM	Intercellular Adhesion Molecule
ICP	Intracranial Pressure
IFN	Interferon
IL	Interleukin
JIP	JNK Interacting Protein
JNK	c-Jun HN_2-terminal Kinase
LPS	Lipopolysaccharide
MAP	Mitogen-activated Protein
MMP	Matrix Metalloproteinase
mRNA	messenger Ribonucleic Acid
NF-κB	Nuclear Factor-κB
NO	Nitric Oxide
O.D.	Optical Density
PAGE	Polyacrylamide Gel Electrophoresis

PBS	Phosphate Buffered Saline
PFA	Paraformaldehyde
PGE_2	Prostaglandin E_2
PMN	Polymorphonuclear leukocyte
PSI	Pressure Per Square Inch
PVDF	Polyvinylidene Difluoride
p-ERK	Phospho-Extracellular Signal-regulated Kinase
p-JNK	Phospho-c-Jun HN_2-terminal Kinase
p-p38	Phospho-p38
ROS	Reactive Oxygen Species
SDS	Sodium Dodecyl Sulfate
SEM	Standard Error of the Mean
TBI	Traumatic Brain Injury
TBS	Tris Buffered Saline
TGF	Transforming Growth Factor
TMB	3,3,5,5'-Tetramethylbenzidine
TNF	Tumor Necrosis Factor
VCAM	Vascular Cell Adhesion Molecule
ZO-1	Zonula-occluden protein-1

Chapter 1

1 Introduction

Traumatic brain injury (TBI) remains to be one of the leading causes of morbidity and mortality in children [1,2]. One component of the brain that may be severely affected following TBI is the blood-brain barrier (BBB). The BBB plays an integral role in the maintenance of homeostasis in the central nervous system and the loss of its normal function can lead to secondary injury to the brain tissue [3]. Although BBB dysfunction is suspected to be one of the pathological consequences of TBI, the mechanisms are poorly understood.

1.1 Traumatic Brain Injury

Every year, millions of people in North America are hospitalized due to traumatic injuries, with over 50 000 cases resulting in death [4]. At present, traumatic injuries remain to be one leading cause of death in children in developed nations [1, 2]. A majority of children hospitalized from trauma suffer an injury to the head, or traumatic brain injury (TBI) and 70% of the trauma-related deaths result from the sustained head injury [2, 4].

Most TBIs occur from falls and motor vehicle collisions [4, 5]. Children and adolescents are more likely to sustain a more severe TBI than adults due to their under-developed skulls, weaker necks, and larger head-to-body proportions [2, 4, 5]. A child's head is disproportionally larger relative to their body size, thereby making them more

susceptible to a more severe brain injury from a given force of impact compared to an adult [2]. Maturing skulls in children also contain less calcification, which provides less protection to the brain tissue [4]. TBIs often have severe outcomes, including death and long-term neurological deficits [6, 7]. The pathology of TBI is still not fully understood, and only supportive treatments are available to reliably improve the long-term outcome for patients suffering from severe trauma.

1.2 Classification of TBI

TBI in patients are highly heterogeneous and depend largely on the type and extent of the traumatic impact to the head. In general, TBI can be classified into two groups: primary and secondary brain injuries [2]. The extent of the primary injury that a person suffers following trauma depends on the magnitude and severity of the impact of trauma that result in structural damage to the brain tissue [2, 5]. Trauma to the head may result from a direct contact or impact loading - when the head comes in contact with another object, or from a non-contact or inertia loading - when the brain experiences rapid acceleration/deceleration motion in the skull [8]. The mechanical strain produced by a TBI can be classified as comprehensive (reduced volume), shear (application of torque, or rotation to a body) or tensile strain (increased length) [9]. The force of impact and the resulting mechanical strain endured by the tissue determines the extent of the primary injury. Primary traumatic brain injuries may include skull fracture, contusion, lacerations, haematoma, diffuse axonal injury, and dural tears from rapid acceleration/deceleration of the head [2,5, 8, 10]. A majority of pediatric trauma

deaths occur shortly after impact due to the severity of the primary injuries sustained by trauma [2].

Traumatic brain injured patients are also prone to suffer from complications arising from their initial trauma, or secondary traumatic brain injuries [2]. Secondary traumatic injuries may include hypoxia resulting from airway obstruction, hypotension due to pulmonary dysfunction and blood loss, dysregulation of carbon dioxide, tissue electrolyte imbalance, accumulation of neurotoxins, inflammation, brain swelling, and increased intracranial pressure [2, 7, 10]. Insufficient management of secondary complications can severely affect the brain tissue and worsen a TBI [2, 6, 11, 12].

1.3 Blood-brain Barrier

A major component of the brain that could be severely affected in a TBI is the BBB. Neurons in the central nervous system (CNS) require a tightly regulated local microenvironment for proper functioning [3, 13]. Maintenance of the CNS environment depends on the BBB [3, 13]. The BBB is found in the microvasculature of the brain and forms a physical barrier between the CNS and circulation [14]. In an average adult human brain, the BBB represents 12-18m^2 surface area of blood-brain exchange [14]. Functions of the BBB include separating central and peripheral pools of neurotransmitters, regulating nutrient and ion exchange across the microvessel, and excluding harmful molecules from entering the brain [14]. Many proteins found in the blood, such as albumin and pro-thrombin can induce cellular activation and injury in the brain parenchyma [14]. The BBB is also capable of protecting the CNS from

circulating neurotoxins, whether endogenous or acquired from the environment [14]. Dysfunctional BBB may lose its ability to properly regulate the movement of substances into the brain tissue, leading to further damage to the brain tissue.

The BBB is composed primarily of cerebrovascular endothelial cells (CVEC) and astrocytes, with smaller numbers of pericytes, and pericytic macrophages [3]. These cells interact with one another as a functional unit that together give rise to the unique features of the BBB. The luminal side of the BBB is lined with specialized CVEC (**Figure 1-1**) [3, 13, 14]. These endothelial cells are unique from other endothelial cells found in the peripheral parts of the body. CVEC act as the "physical barrier" between the blood and the CNS, and restrict the movements of cells and various molecules across the microvessels. CVEC develop intercellular tight junctions, which contain high levels of occludin, claudin-5, and zonula-occluden protein 1 (ZO-1), that restricts paracellular movements across the vessel and infer the characteristically low permeability of the BBB [13]. Relative to peripheral capillaries, the cerebral microvasculature are 50 to 100 times tighter [15]. In addition, CVEC lack cellular fenestrae and essentially have no pinocytotic activity that together, further restricts molecular transport across the endothelium [13, 16]. Small gaseous molecules (i.e. O_2 and CO_2) and lipophilic molecules can freely diffuse through the plasma membrane, but most transcellular transport of nutrients, waste, and other hydrophilic molecules require specific transport proteins on CVEC surface [13]. Thus CVECs of the BBB play an essential role in regulating the exchange of substances between the blood and the CNS.

On the basolateral side of the endothelium, a basement membrane surrounds the microvessels. (**Figure 1-1**). Beyond that, the BBB microvasculature is almost entirely

covered by supporting astrocyte processes [17]. Perivascular astrocytes project their specialized endfeet to surround the cerebral microvasculature (**Figure 1-1)** [13]. Astrocyte endfeet are in close contact with CVEC and are believed to induce key characteristics of the endothelium and further enforce the low permeability of the microvasculature [13, 16, 18]. They also are key mediators for cell-to-cell communications between neurons and the microvessels [17]. Furthermore, overlapping astrocyte processes covering the cerebral vasculature is also believed to play a significant role control of localized blood flow and in restricting water influx into the brain parenchyma [17]. There is an abundant expression of water channels, Aquaporin 4 (AQP4) on astrocytic endfeet that are involved in regulating ion and water movements across the vasculature [13, 19]. Thus, astrocyte endfeet play a major role in the proper functioning of the BBB [13, 16, 18, 19].

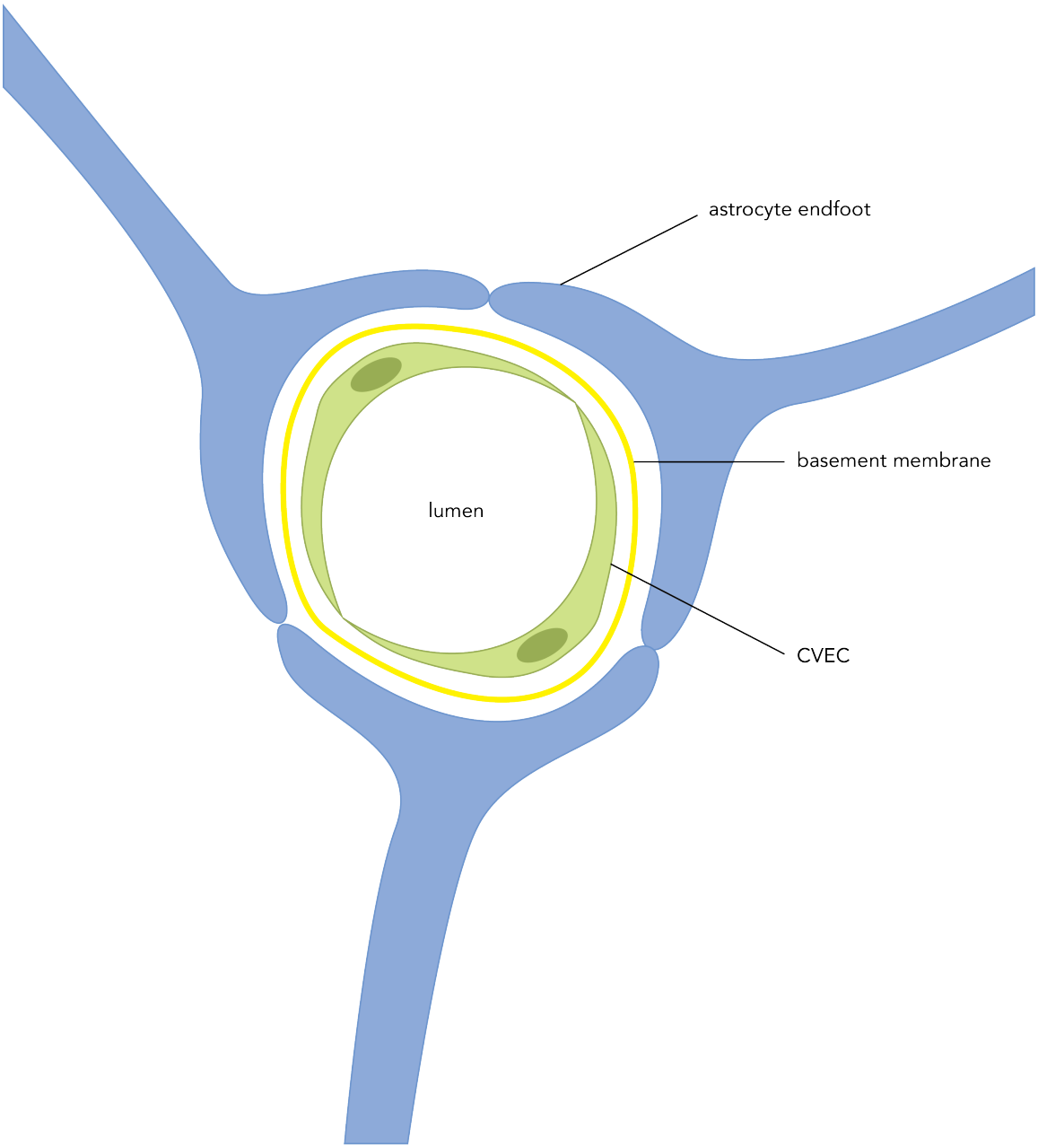

Figure 1-1 Simplified Schematic Diagram of the Blood-brain Barrier. The blood-brain barrier (BBB) is a specialized anatomical function found unique in the microvasculature of the brain. Specialized cerebrovascular endothelial cells (CVEC) line the lumen of the vasculature. A basement membrane surrounds the blood vessel, which are subsequently ensheathed by the end-foot processes of perivascular astrocytes. Together, they function to infer a low permeability of the blood vessel and restrict the exchange of substances between the circulation and the brain parenchyma.

1.4 Astrocyte-Endothelial Cell Coupling

Proper function of the BBB depends on intimate interactions between the cellular components of the vasculature and of the CNS [13, 19]. Perivascular astrocytes project their endfeet to almost entirely cover the basolateral side of the microvasculature [13, 16, 19]. Typically, perivascular astrocytes and endothelial cells are in constant communication and regulate the function of one another [13, 19]. In an *in vitro* co-culture system, astrocytes can induce endothelial cells to express many BBB-specific phenotypes, including the formation of more restrictive tight junctions, as well as the expression and polarization of CVEC selective transporter proteins [13, 19]. Induction of BBB-specific characteristics depends on cell-cell contact and the release of local mediators [15]. Astrocytes release a number of paracrine mediators, including transforming growth factor-β (TGF-β), glial-derived neurotrophic factor (GDNF), basic fibroblast growth factor (bFGF), and angiopoetin 1 (ANG1), that can induce endothelial cells to express BBB phenotypes (**Figure 1-2)** [13, 15, 19]. In turn, endothelial cells can also affect astrocyte phenotypes. In a co-culture, endothelial cells can stimulate astrocytes to grow, polarize, and produce laminin – which forms a structure resembling a basement membrane [15]. The disturbances or loss of astrocyte-endothelial interactions may severely affect the integrity of the BBB. Several pathological conditions have been associated with the disturbance between endothelial cells and glial cell interactions [13]. For example, the capillaries in glial tumors exhibit increased vascular permeability due to the lack of inductive factors secreted by astrocytes [13].

Perivascular astrocytes also function to mediate communication between neurons and the vasculature [13, 19]. Together with CVEC, astrocytes associate with

neurons to form a neurovascular unit to maintain proper blood flow in the capillaries to maintain CNS homeostasis [13, 19]. Increased neural activity is accompanied by increased in localized cerebral blood flow, known as functional hyperemia [20]. Functional coupling between neural activities and the response of the microvasculature maintains the balance between energy supply and metabolic demand [15, 19].

During a synaptic activity, neurons communicate with astrocytes to signal the endothelium for increased blood flow to supply oxygen, energy supply, and removal of toxic by-products [15, 19]. Unlike larger blood vessels, the capillaries lack smooth muscles for mediating vasodilation and vasoconstriction to regulate local blood flow. Instead, dynamic changes in local capillary vasodilation/vasoconstriction are mediated by perivascular astrocytes [15, 19, 20]. Within seconds of synaptic activities, there is a transient wave of intracellular Ca^{2+} in astrocytes, which stimulates the release of vasodilation/vasoconstriction factors [20]. These mediators include cyclooxygenase (COX) 1 and 2 metabolites such as prostaglandin E_2 (PGE_2), epoxyeicosatrienoic acid (EETs), nitric oxide (NO) and adenosine [20].

Furthermore, astrocytes are also involved in regulating glucose uptake across the capillaries [15]. Neuronal activity up-regulates GLUT1 transporter activities on perivascular astrocyte end-feet via Na^+ and Ca^{2+} messenger pathways to increase glucose availability for neurons (**Figure 1-3**) [15]. Functional hyperemia to match the cerebral blood flow to the demand of neural activity occurs rapidly (within seconds) and likely requires intimate contact between perivascular astrocyte endfeet and endothelial cells [20]. Disruption of astrocyte-CVEC coupling can lead to the

dysregulation of cerebral blood flow and further exacerbate a neurological pathology [15, 19].

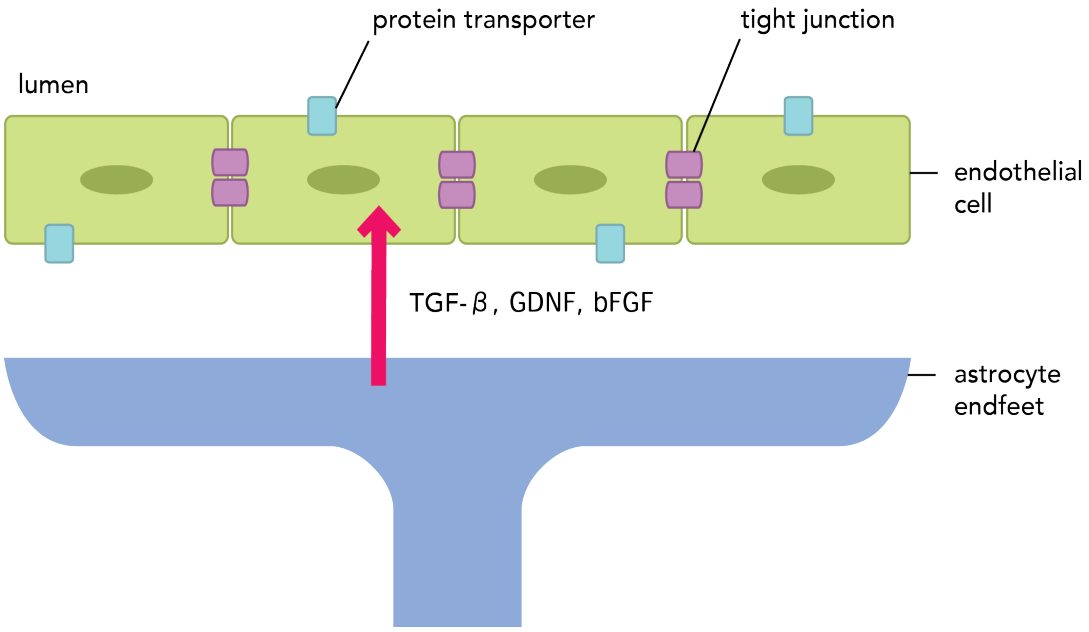

Figure 1-2. Perivascular Astrocyte Induces BBB Phenotype in Endothelial Cells. Astrocyte and endothelial cell coupling is important in the induction of BBB phenotype in the brain capillaries. Astrocyte endfeet that are in contact with cerebral endothelial cells release factors such as TGF-β, GDNF and bFGF to induce tightening of intercellular tight junctions between endothelial cells, as well as expression and polarization of selective protein transporters. Astrocytes are essential in inducing and maintaining the low and selective permeability of the BBB [13, 15, 19].

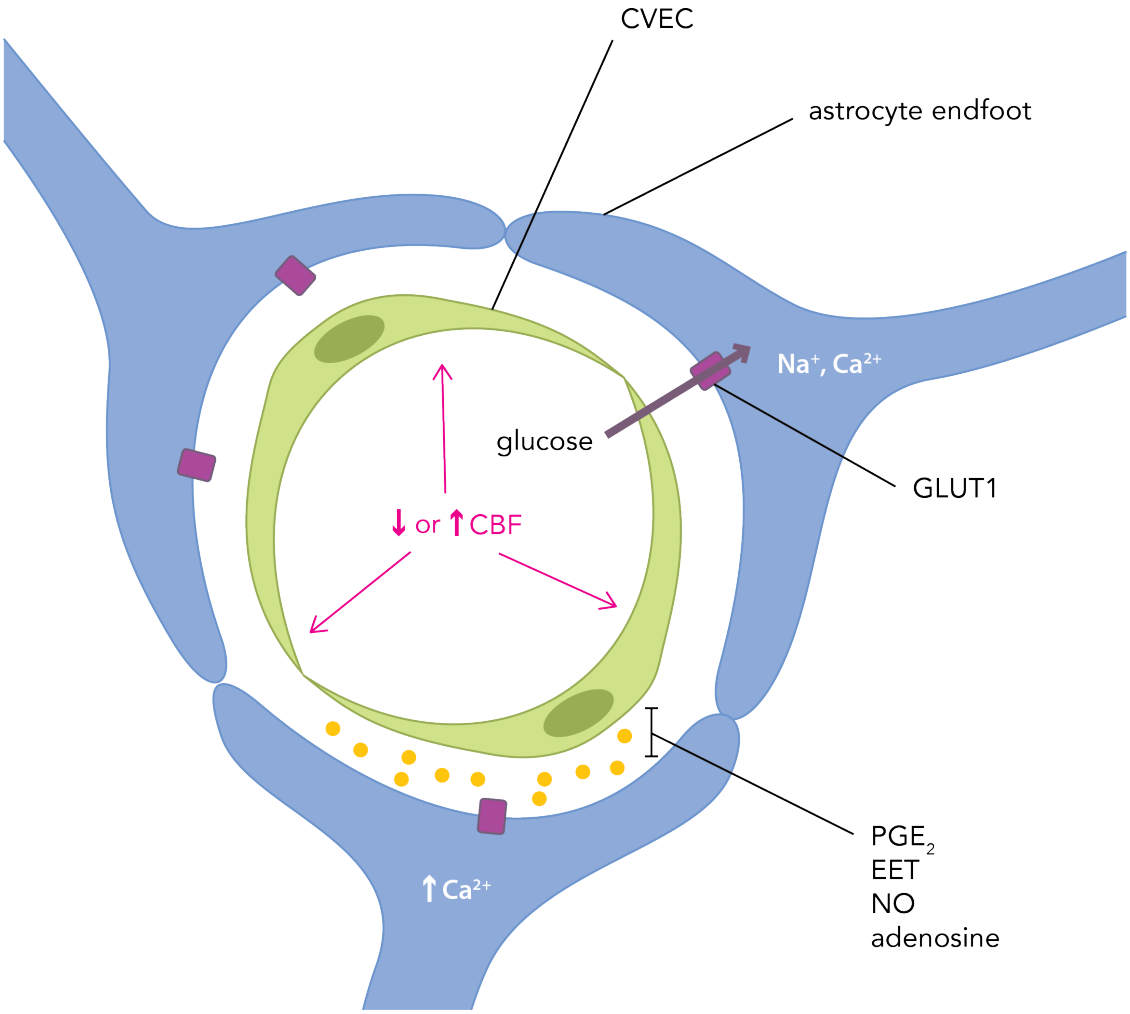

Figure 1-3 Role of Perivascular Astrocytes in Regulating Cerebral Blood Flow (CBF). Astrocytes play an integral role in regulating capillary vasodilation and vasoconstriction to supply neurons with proper energy supply. Upon neural activation, there is a transient increase in intracellular Ca^{2+} that signals astrocytes to release vasodilating or vasoconstricting factors such as PGE_2, EET, NO and adenosine. Na^+ and Ca^{2+} also up-regulates GLUT1 activities on astrocyte endfeet to facilitate glucose transport across the vasculature. Thus the coupling of astrocyte endfeet to the cerebrovasculature is essential in neural-vascular communication and regulating local CBF for functional hyperemia [15, 19, 20].

1.5 Pathology of TBI

Post-mortem examination of the brain of TBI victims reveal morphological changes to the components of the BBB [21]. Assessment of human brains following TBI revealed regions of reactive astrocytes and perivascular hemorrhage [18]. There are also regions of enlarged perivascular space and swelling of astrocytes [21, 22]. Observations of injured brains revealed changes in perivascular astrocyte morphology. These changes range from separation of astrocyte endfeet from the basement membrane of the microvasculature to fragmented astrocytic processes with extensive areas of capillary basement membranes absent of astrocyte coverage [21]. This suggests that there are trauma-induced changes in perivascular astrocyte morphology, which may be involved in the pathology of TBI.

Aside from the dysfunction associated from the mechanical impact of trauma, the brain is also prone to the inflammatory effects of trauma that may worsen a TBI. The CNS has long been considered to be an "immune privileged" site. Under a non-pathological condition, few immune cells are found in the brain parenchyma [3, 23]. The exclusion of circulating immune cells, such as polymorphonuclear leukocytes (PMN) is largely due to the presence of the BBB. In rat models of TBI, there appears to be an accumulation of PMN in the brain that correlates with the severity of post-traumatic injury [24, 25]. Overwhelming PMN infiltration in the brain may exacerbate TBI by propagating neuroinflammation and contributing to the formation of edema [24].

Recruitment of PMN in the brain following injury is likely facilitated by a trauma-induced change in CVEC function. Under a normal physiological condition,

CVEC of the BBB form a physical barrier that restricts PMN from entering the brain parenchyma [3, 16, 24]. Traumatic injuries may induce up-regulation of enzymes (i.e. matrix metalloproteinases) that can degrade the matrix components between cells, thereby making the vessels "leaky" with increase its vascular permeability [26]. CVEC may also increase the expression of surface adhesion molecules (i.e. E-selectin, Vascular Cell Adhesion Molecule (VCAM), and Intercellular Cell Adhesion Molecule (ICAM), which up-regulates CVEC interactions (e.g. rolling/adhesion) with circulating PMN and facilitates PMN migration across the vasculature [11, 27, 28]. Although neuroinflammation has been well documented following TBI [7, 11], PMN infiltration into the brain in *humans* following traumatic injury remains unclear and continues to be under investigations.

1.6 Astrocyte Cellular Response to Injury

Astrocytes project their endfeet over the basal membrane and surround the entire vessel of the BBB (**Figure 1-1**) [16]. They come in close contact to CVECs and are believed to be involved in the regulation of BBB function [13, 16]. Loss of contact or uncoupling between the astrocyte-CVEC units may disrupt cell-cell communications, which may lead to the dysfunction of the BBB.

The physical (mechanical) impact of TBI can severely affect the morphology and function of astrocytes. Multiple studies have been conducted to study the effects of TBI on astrocytes using *in vivo* animal models and *in vitro* stretch injuries, scratch injuries, cell disruption techniques, and fluid percussion models using animal-derived

cell culture [9, 26, 29, 30, 31, 32]. In an *in vitro* model of TBI, primary rat astrocytes have exhibited increasing markers of injury correlating with greater stretch/concussive injury [9]. Injured rat astrocytes exhibit the loss of plasma membrane integrity and a change in cellular morphology [9]. Whereas uninjured rat astrocytes exhibit polygonal shape and form confluent monolayers, moderately injured cells (30% stretch) became swollen, and severely injured cells (55% stretch) retracted and became stellate-shaped [9]. The changes in morphologies of injured rat astrocytes are also accompanied with swelling of the mitochondria and destruction of astrocyte glial filaments [9. 33].

In addition to changes in cell morphologies, injured astrocytes may exhibit other markers of cellular activation. A major focus has been on calcium-dependent astrocyte response to stretch injury [34, 35]. Studies using rat astrocytes *in vitro* have reported rapid and transient increase in intracellular calcium after stretch injury [32], along with generation of free radicals [33, 36], nitric oxide production [33] and mitogen-activated protein (MAP) kinase activation [33, 37]. Despite ongoing research, the pathology of astrocyte injury following trauma and its contribution to the development of BBB dysfunction and breakdown post-injury has yet to be explained.

1.7 CVEC Cellular Response to Injury

The luminal surface of the BBB is lined with CVEC that play a significant role in maintaining the low permeability of the microvasculature [3]. These specialized endothelial cells form the first barrier between the blood and the brain parenchyma, and the loss of CVEC intercellular tight junctions, dysregulation of transcellular transport,

and increased interactions with circulating immune cells can lead to an influx of circulatory components into the CNS [1, 3, 27]. Disruption of the CVEC barrier may be directly due to the impact force of trauma or as indirectly as a secondary consequence mediated by neighbouring injured cells (i.e. astrocytes) [3].

Following a mechanical or biochemical insult, endothelial cells exhibit acute responses that occur within minutes, which does not depend on de novo mRNA expression and synthesis of new proteins [28]. Acute cellular response typically involves protein modifications, such as phosphorylation of signaling molecules. Rapid responses such as activation of signaling pathways can lead to a long term or delayed change in cell phenotype. Delayed response to insults typically involves mRNA transcription and synthesis of new proteins. In endothelial cells, a long-term or delayed response to injury or stress typically includes expression of surface adhesion molecules to facilitate interactions with circulating immune cells, secretion of local inflammatory mediators and production of various growth factors [28].

A classic signaling pathway typically involved in endothelial cells following stress or injury is the nuclear factor-κB (NF-κB) pathway. The transcription factor NF-κB is activated by various stimuli including inflammatory factors such as tumor-necrosis factor- (TNF-) α and β, interleukin- (IL-) 1β, as well as ROS and lipopolysaccharide (LPS) [38]. NF-κB consists of multiple subunits: e.g. p50 and p65 and I-κB. In its inactive form, p50 and p65 (or their precursor p105/p100) form complex with I-κB in the cytoplasm. Following activation, the I-κB becomes phosphorylated, then subsequently ubiquitinylated and degraded, allowing p50 and p65 hetero- and/or homo-dimers to translocate to the nuclei where they can initiate

transcription of the targeted genes [38]. Among the genes transcribed by activated NF-κB include various inflammatory mediators (i.e. cytokines and chemokines) and endothelial cell surface adhesion molecules [38, 39]. Other signal transduction pathways known to be activated in response to stress and injury involves the mitogen-activated protein (MAP) kinase family.

1.8 MAP Kinase

One major signal transduction pathway that has been studied extensively in various cell types and pathological conditions is the MAP kinase pathway. MAP kinases respond to extracellular cues and induce an internal cellular response [40, 41]. MAP kinase responds to various stimuli, which includes cytokines, growth factors, hormones, environmental stress and injury [41]. MAP kinases govern various cellular functions, including various gene transcriptions, protein synthesis, cell growth, differentiation and apoptosis [41].

In mammals, the three members of the MAP kinase family have been well implicated in response to stress and injury: The Extracellular signal-regulated kinase (ERK), the c-Jun NH_2-terminal kinase (JNK) and the p38 MAP kinases. Studies have reported the activation of ERK and p38 MAP kinases in response to traumatic injuries in animal models [25, 33, 40, 42]. ERK and p38 are typically activated by stress and cytokines [41].

The exact mechanism of signal transduction pathway from a mechanical injury (i.e. concussion) to the activation of MAP kinase in astrocytes and CVEC is not fully

understood. MAP kinase activation is regulated by a family of MAP kinase kinase (MAP2K), which in turn is activated by a family of MAP kinase kinase kinase (MAP3K) [41]. In injured cells, the MAP kinase signaling cascade may be initiated in response to extracellular ATP (via P2Y G protein-coupled receptors), reactive oxygen species (ROS), nitric oxide (NO), and intracellular Ca^{2+} wave– all of which markedly increased following mechanical injury [33, 34, 35, 37, 43].

Following trauma, ERK and p38 activations lead to secretions of inflammatory factors, up-regulation of matrix metalloproteinases (MMPs), and change in cellular morphology [25, 33, 40, 42]. The JNK signaling pathway is activated in response to environmental stress, toxins, ischemic reperfusion injury, pro-inflammatory cytokines, and mechanical shear stress [41]. JNK activation can lead to a change in cell morphology, secretions of inflammatory mediators, and cellular apoptosis [41]. MAP kinase is also involved in regulating cell shapes and cytoskeleton stability through the phosphorylation of actin- and microtubule-associated proteins [44]. Dynamic changes to the cytoskeleton (i.e. actin assembly/disassembly) may be accompanied by the modification of integrin-mediated focal adhesions [45, 46]. Integrin acts as a bridge between actin cytoskeleton and extracellular matrix (ECM) protein for cell adhesion [46]. Alterations of integrin-ligand density and organization affects cell surface adhesion to ECM and facilitate in cell spreading and retraction [46].

1.9 Rationale and Objective

Currently, the pathology of TBI is not fully understood, but trauma may disrupt astrocyte and CVEC coupling that is critical for normal brain function. Our study employed an *in vitro* model of the BBB using either primary human astrocytes (HA) or a well-characterized immortalized human cerebral microvascular endothelial cells (hCMEC/D3). By assessing the effects of trauma on astrocytes and CVEC individually, we can further understand the role of each major component of the BBB in the pathology of a TBI.

To simulate a TBI *in vitro*, the Cell Injury Controller II (Virginia Commonwealth University Medical Center, Richmond, VA) delivers a regulated, pressurized air pulse to culture wells that induces a biaxial stretch injury (i.e. concussive injury) to cells grown on a flexible membrane. This type of injury mimics both a concussive and stretch injury experienced by tissues during a rapid rotational acceleration/deceleration head movement [9]. In this study, either HA or hCMEC/D3 monolayer was subjected to a single, 50 milliseconds, rapid stretch that translates to a single concussive injury [9]. The TBI model employed in this study allows for a homogenous and repeatable injury.

Clinical studies in patients with TBI revealed that concussive injury induces morphological change in astrocytes (i.e. retraction of astrocyte endfeet from vascular basement membrane) [21]. In parallel, an increase in PMN accumulation in rat brains following injury has been demonstrated, suggesting increased PMN-CVEC adhesive interactions [7, 24, 25] In our study, we aimed to determine the cellular responses of either HA or hCMEC/D3 following a single concussive injury *in vitro*.

Objectives:

(1) To determine whether a concussive injury induces changes in cellular morphology of either HA or hCMEC/D3 monolayer.

(2) To determine the role of MAP kinases in HA and hCMEC/D3 response following a concussive injury.

(3) To determine whether there is an up-regulation of pro-adhesive phenotype in concussively injured hCMEC/D3.

Our study strictly employs the use of *human* tissues (ie. human astrocytes, human CVEC, and human PMN), which may have a strong translational aspect to further understand the pathology of TBI in humans, and can potentially lead to the development of therapies for TBI patients.

1.10 Hypothesis

We hypothesize that:

1) Concussive injury induces morphological changes in either HA or hCMEC/D3.
2) Concussive injury induces activation of MAP kinases in HA and hCMEC/D3.
3) Concussive injury to hCMEC/D3 induces PMN adhesion

Chapter 2

2 Methodology

We employed the use of either HA or hCMEC/D3 to assess for cellular response following a concussive (i.e. mechanical) injury *in vitro.* We assessed for functional changes induced by a severe concussive injury to cultured HA or hCMEC/D3, as well as determining the underlying mechanisms involved in mediating cellular response following injury.

2.1 Traumatic Brain Injury Model *in vitro*

An *in vitro* model of TBI was employed using the Cell Injury Controller II (Virginia Commonwealth University Medical Center, Richmond, VA), an electronically controlled pneumatic device capable of inducing regulated and repeatable trauma to cell culture. The Cell Injury Controller II delivers a pulse of controlled gas pressure to deform a flexible membrane fitted at the bottom of a commercially available Bioflex® culture wells to induce a concussive injury *in vitro* (Flexcell International Corp, Hillsborough, NC). In our experimental approach, the Cell Injury Controller II delivered a 50-millisecond burst of gas into the culture well to induce a rapid membrane deformation (**Figure 2-1**). The Cell Injury Controller allows for delivered pressure adjustments to produce varying degrees if injury: “mild” (20% deformation with 1.8 peak PSI), “moderate” (35% deformation with 2.7 peak PSI) and “severe” (55%

deformation with 4.0 peak PSI) concussive injuries. The amount of deformation reported refers to the maximum percentage increase in surface area of the flexible membrane as it stretched in response to the machine-delivered positive pressure in the culture well. During the deformation of the membrane, cultured cells adhering to the membrane surface experienced a biaxial stretch that translated to a mild, moderate, or severe concussive injury (single hit), simulating a rotational, acceleration/deceleration-type trauma *in vitro* [9].

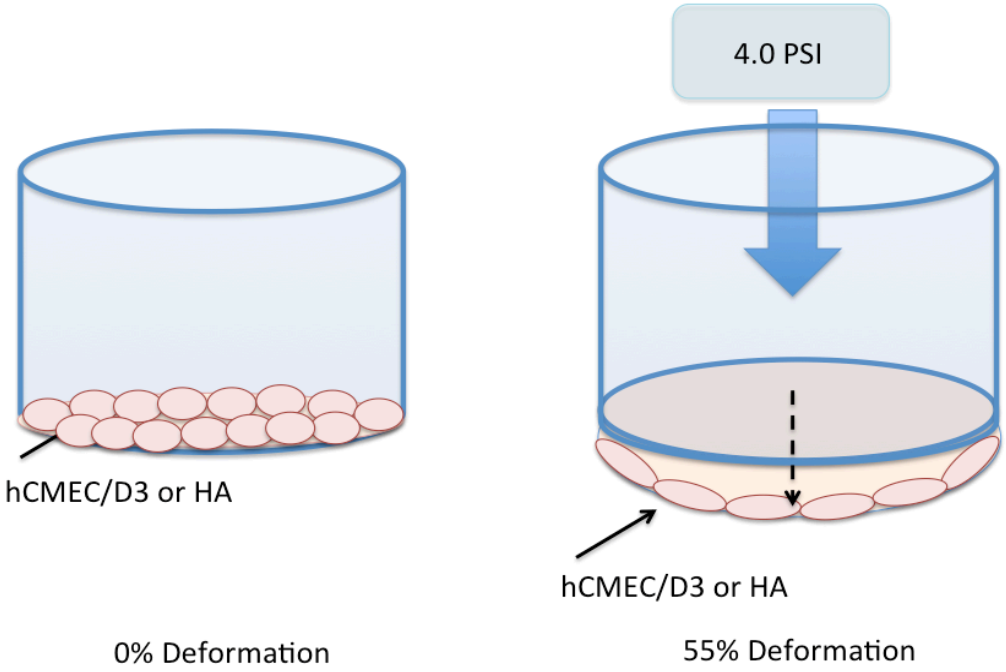

Figure 2-1. Severe Concussive Injury modeling TBI *in vitro*. HA or hCMEC/D3 were grown on a fibronectin-coated flexible membranes of Bioflex® culture wells. The Cell Injury Controller II delivers a positive pulse of air (measured as 4.0 PSI/well) into the culture well and deforms the flexible membrane (at 55% stretch). In turn, cells adhering to the membrane experience a biaxial shear strain (or stretch-type injury) that translates to a "severe" concussive/traumatic injury.

2.2 Human Astrocytes

Primary human astrocytes (HA; isolated from the cerebral cortex of a single donor) were purchased from ScienCell™ Research Laboratories (Carlsbad, CA). HA were grown on fibronectin-coated Bioflex® culture plate (Flexcell International Corp, Hillsborough, NC) in VascuLife® cell culture medium supplemented with recombinant human epidermal growth factor (5 ng/mL), L-glutamine (5 mM), ascorbic acid (50 μg/mL), fetal bovine serum (4%), penicillin (100 IU/mL) and streptomycin (100 μg/mL). HA were grown in 37°C with 5% CO_2 until cell monolayer reaches confluency. Passages 2-7 were used for experimentations.

2.3 Human Cerebrovascular Endothelial Cells

This study employs a stable, fully characterized immortalized human cerebrovascular endothelial cell line, hCMEC/D3, provided to our lab by Dr. Pierre-Oliver Couraud (INSERM, Paris, France). Briefly, primary human brain endothelial cells were immortalized by lentiviral transduction of hTERT and SV40 large T antigen as previously described [47]. hCMEC/D3 line exhibit phenotypes of fully-differentiated primary human brain endothelial cells *in vitro*, including the capacity to up-regulate the expression of surface adhesion molecules in response to inflammatory mediators, formation of tight junctions between cells, and exclusion of drugs across a monolayer [47, 48]. hCMEC/D3 were grown on fibronectin-coated Bioflex® culture plates (Flexcell International Corp, Hillsborough, NC) in VascuLife® Endothelial Cell

Growth Supplement (EnGS) cell culture medium supplemented with recombinant human EnGS (0.2%), recombinant human epidermal growth factor (5 ng/mL), L-Glutamine (10 mM), hydrocortisone hemisuccinate (1.0 μg/mL), heparin sulfate (0.75 μg/mL), ascorbic acid (50 μg/mL), fetal bovine serum (5 %), penicillin (100 IU/mL) and streptomycin (100 μg/mL). hCMEC/D3 were grown in 37°C with 5% CO_2 until the cell monolayer reaches confluency.

2.4 Astrocyte Monolayer Retraction

Confluent HA grown on a fibronectin-coated Bioflex® plate form a dense cell monolayer. Following a severe concussive injury, HA monolayer appears disrupted with increased appearance of spaces between cells. To assess HA monolayer integrity following a stretch injury, we designed an assay to allow us to quantify a monolayer retraction. To do so, we selected a cell-permeable dye that would provide a uniform, whole-cell staining of live cell culture.

HA grown on fibronectin-coated Bioflex® plate were pre-loaded with 20 μM 5,6-carboxyfluoroscein diacetate (CFDA; Molecular Probes, Eugene, OR) in Vasculife® astrocyte culture medium for 30 minutes at 37°C. Following 2X wash with warm PBS, cells received: (1) no injury, (2) mild injury (20% deformation), (3) moderate injury (35% deformation) or (4) severe concussive injury (55% deformation), and further incubated for another 30 minutes. Subsequently, images of the uninjured and injured HA monolayers were captured by fluorescent microscopy (Zeiss Axiovert 200M Inverted Microscope; Carl Zeiss Canada Ltd., Toronto, Canada). 4 random fields

of view for each treatment were captured at 33X magnification. Cell monolayer retraction was assessed by quantifying the percentage of cell coverage in each image measured by autothresholding the total surface area covered by cells (visible under fluorescence) using an ImageJ software.

2.5 Quantification of Astrocyte Detachment

To determine whether there is significant HA detachment following severe concussive injury, we quantified the number of cells present in the culture media following a severe concussive injury. HA were grown on fibronectin-coated Bioflex® culture well until the monolayer reached confluency. Cells were washed 1X with warm PBS and placed in 300 µL of fresh culture media per well. HA were subjected to a severe concussive injury (55% deformation) and incubated for 30 minutes at 37°C. Subsequently, the culture media from triplicate wells of uninjured and injured HA were collected into microtubes. Uninjured and injured cell media samples were centrifuged at 20 000 g for 10 minutes and each pellets were resuspended in 75µL of cold PBS. Cells were placed in a much smaller volume (12X concentrated) relative to the original sample volume to allow for a more accurate cell counting. The number of cells in each sample was counted using a Haemocytometer (Hausser Scientific, Horsham, PA) and expressed as the number of cells detached per monolayer.

To determine the total number of HA in a confluent monolayer, confluent cells were fixed in 3% paraformaldehyde (PFA; Bioshop Canada Inc, Burlington, Canada) in PBS for 15 minutes and permeabilized in 0.1% Triton X-100 (Sigma Aldrich, St. Louis,

MO) in PBS for 10 minutes. Cellular nuclei were stained with Hoechst 33342 nuclear stain (Molecular Probes, Eugene, OR) for 2 minutes and images were captured by fluorescent microscopy (Zeiss Axiovert 200M Inverted Microscope; Carl Zeiss Canada Ltd., Toronto, Canada). The number of cells (with respect to the number of nuclei) in a 10 000 μm^2 field of view were counted from 4 confluent HA monolayers to determine the total number of cells on one a Bioflex® culture well (1.96 cm^2 growth area per well).

2.6 MAP Kinase Activation Following Severe Injury

Activations of MAP kinases, ERK, JNK and p38 were assessed by phospho-ERK 1/2, phospho-JNK 1/2 and phospho-p38 Western blotting. Confluent HA or hCMEC/D3 were grown on fibronectin-coated Bioflex® plate. Uninjured and severely injured cells were incubated for 30 minutes, then washed with cold PBS supplemented with 0.4 mM sodium orthovanadate (Sigma-Aldrich, St. Louis, MO), a phosphatase inhibitor. Following the wash, cells were lysed in 200 µL hot sodium dodecyl sulfate (SDS)-electrophoresis sample buffer. Samples were sonicated, then boiled for 5 minutes at 95°C. Uninjured and injured cell samples were then subjected to a 12% SDS-polyacrylamide gel electrophoresis (PAGE), and proteins were transferred overnight to a BioTrace™ polyvinylidene difluoride (PVDF) membrane (Pall Corporation, Port Washington, NY).

The membranes were blocked in 5% skim milk with 0.1% Tween in tris-buffered saline (TBS) for 1 hour. Then, they were incubated for 1 hour at room

temperature with mouse monoclonal antibody against phospho-ERK1+ERK2 (Clone MAPK-YT; Abcam Inc., Cambridge, UK), rabbit polyclonal antibody against phospho-JNK1+JNK2 (Abcam Inc., Cambridge, UK) or rabbit monoclonal antibody against phospho-p38 (Clone E229; Abcam Inc., Cambridge, UK) in 2% skim milk in TBS. The membranes were then incubated with corresponding horseradish peroxidase (HRP)-conjugated secondary antibodies (Invitrogen, Carlsbad, CA) in 2% skim milk in TBS. For the protein loading control, membranes were also probed with mouse monoclonal antibody against Glyceraldehyde-3-phosphate dehydrogenanse (GAPDH; Clone 6C5; Abcam Inc., Cambridge, UK). Levels of phospho-ERK, JNK, and p38 proteins were standardized to GAPDH rather than its corresponding total MAP Kinase protein levels to avoid membrane stripping and loss of protein signal quality associated with the latter technique. Bound target antibodies were visualized using enhanced chemiluminescence detection (2.5 mM Luminol, 0.4 mM p-Coumaric acid, 0.02% hydrogen peroxide in 100 mM Tris buffer; Sigma-Aldrich, St. Louis, MO). Images of the immunoblots were captured using a MicroChemi imaging system (FroggaBio, Toronto, Canada) and band quantifications were done using GelQuant Pro Software (FroggaBio, Toronto, Canada).

2.7 JNK Inhibitors

To determine whether there is a link between JNK 1/2 activations in HA with monolayer retraction, changes in injured HA morphology was assessed in the presence of JNK inhibitors. We employed two commercially available JNK inhibitors, SP600125 (Sigma Aldrich, St. Louis, MO) and SU3327 (Tocris Bioscience, Bristol, UK).

SP600125 is a cell permeable, selective inhibitor of JNK-1, -2 and -3, and has been widely used with various cell types [42, 49, 50]. SP600125 is a reversible, adenosine triphosphate (ATP) competitive inhibitor [51], which prevents JNK activation by blocking the ATP binding site on the JNK molecule [52]. SU3327 is a more recently developed selective, competitive JNK inhibitor that prevents protein-protein interactions between JNK and JNK Interacting Protein (JIP) [53], a scaffold protein responsible for regulating JNK signaling [41].

HA monolayer retraction was assessed as described above. Following CFDA staining, cells were washed with warm PBS and placed in fresh culture medium. Cells treated with the JNK inhibitors were supplemented with 25μM of SP600125 or SU3327. The concentrations of JNK inhibitors were selected according to currently published literatures that closely resemble our experimental settings [33, 42, 51, 52, 53]. HA were incubated with the JNK inhibitors for 10 minutes prior to injury. Monolayer retraction in HA with or without the JNK inhibitors were assessed 30 minutes following a severe concussive injury.

2.8 Assessment of Endothelial Cell Pro-adhesive Phenotype

Human polymorphonuclear leukocytes (PMN) were isolated from venous blood of a healthy adult donor immediately prior to each experiment. 10 milliliters of whole blood was collected into a syringe supplemented with 10 U/mL heparin (Leo Pharma Inc., Thornhill, Canada) and transferred into 5 mL of 3% Dextran in phosphate buffered

saline (PBS) to give a final concentration of 1% Dextran/blood mixture. The mixture was gently inverted 10 times to allow even mixing, followed by a 25 minutes rest at room temperature to allow for red blood cell sedimentation. The PMN-containing upper blood plasma fraction was then transferred and layered on top of 5 mL leukocyte separation medium (1.077 g/mL density Histopaque®-1077; Sigma-Aldrich, St. Louis, MO). Samples were then centrifuged at 400g for 30 minutes at 4°C. Following centrifugation, the supernatant was aspirated, and the PMN-containing pellet was resuspended in 15 mL cold hypotonic buffer to lyse remaining red blood cells (8.30 g/L NH_4Cl, 1 g/L $KHCO_3$, 0.14 mM EDTA; pH 7.2). Following a 5 minutes incubation on ice, samples were centrifuged at 320 *g* for 5 minutes at 4°C. The supernatant was once again aspirated, and the PMN pellet was resuspended in 1 mL cold PBS. The number of PMN recovered was counted using a hemacytometer (Hausser Scientific, Horsham, PA) and cells were kept on ice until immediately before use.

Freshly isolated PMN were labeled with radioactive probe, Chromium-51. Five μCi of Chromium-51 (^{51}Cr; CJS4, CJS11, Amersham Plc, Buckinghamshire, UK) were added per 1 X 10^6 PMN in PBS enriched with 1 mM glucose and incubated at room temperature for 40 minutes. ^{51}Cr-labelled PMN (^{51}Cr-PMN) were washed 2X and resuspended in cold PBS, then kept on ice until use.

Confluent hCMEC/D3 grown on fibronectin-coated Bioflex® in Vasculife® culture medium were subjected to no injury or severe concussive injury and incubated for 4 hours. Subsequently, hCMEC/D3 were washed 1X with warm culture medium and received fresh culture medium. ^{51}Cr-PMN (1 X10^6 cells/well) were added to the hCMEC/D3 monolayer, and cells were further incubated for another 30 minutes at

37°C. Following incubation, cells were washed with warm PBS to remove non-adhering ^{51}Cr-PMN. Remaining cells in the well were lysed with 1M NaOH. Radioactivity levels in the cell lysate samples were measured using an automatic gamma ray counter (Wallac 1480 Wizard™ 3"; Turku, Finland). PMN adhesion to hCMEC/D3 monolayer was presented as percent of PMN adhesion (% CPM in sample relative to total ^{51}Cr-PMN CPM added).

2.9 NF-κB Activation

The relative activation of NF-κB in hCMEC/D3 following severe concussive injury was assessed using a PathScan® Phospho-NF-κB p65 (Ser536) Sandwich ELISA kit (Cell Signaling Technology, Inc., Danvers, MA). The assay was performed according to the protocol provided by the manufacturer. Confluent hCMEC/D3 grown on fibronectin-coated plastic culture well plate were subjected to a severe concussive injury and incubated for 1 hour. Subsequently, cells were washed with cold PBS and lysed with 1x Cell Lysis Buffer (provided by manufacturer) plus 1mM PefaBloc® SC (Sigma-Aldrich, St. Louis, MO). Cell lysates were sonicated, and following a 10 minute 20 000g centrifugation, the sample supernatant were retained. 50 µL of each sample was diluted at 1:1 ratio with a Sample Diluent provided in the kit, and transferred into a Phospho-NF-κB p65-antibody coated-microwell. The microwell plate was incubated overnight at 4°C. Following incubation, the contents of the plate were discarded and the wells were washed 4X with a Wash Buffer (from kit). 100 µL of detection antibody was added into each microwell and the plate was incubated for 1 hour at 37°C.

Subsequently, the detection antibody was removed and the wells were washed 4X with Washing Buffer. 100 µL of HRP-linked antibody was then added into each microwell and the plate was incubated for 30 minutes at 37°C. The contents in the plate were removed and the wells were washed 4X with Washing Buffer. Lastly, 100 µL of TMB substrate was added into each microwell, and following 10 minutes of incubation at 37°C, 100 µL of STOP Solution was added per well. Results of the assay were measured spectrophotometrically using a Bio-Rad 680 Microplate Reader (Bio-Rad Laboratories, Hercules, CA). The absorbance was read at 450 nm and expressed as optical density (O.D) measured. The value of O.D. corresponds to levels of phospho-NF-κB p65 detected in each sample.

Chapter 3

3 Results

Either HA or hCMEC/D3 monolayers were subjected to concussive injury *in vitro* and assessed for changes in cellular morphology with respect to cellular retraction. MAP kinase activation in HA and hCMEC/D3 were assessed using Western blots of phosphorylated JNK 1/2, ERK 1/2, and p38. Severe concussive injury to HA appeared to induce JNK 1/2 activation at 30 minutes post-injury, which correlates to the appearance of monolayer retraction (**Figures 3-1 to 3-8**). Selective JNK inhibitors were employed to determine the role of JNK 1/2 in mediating injury-induced HA monolayer retraction (**Figures 3-9 to 3-10**).

Unlike HA, hCMEC/D3 monolayer does not appear to be affected by a severe concussive injury with respect to its cellular morphology (**Figure 3-1**). To investigate other aspects in which hCMEC/D3 respond to severe concussive injury, we assessed whether there is increased PMN adhesion to injured hCMEC/D3 using radioactive-labeled PMN (**Figure 3-11**). Furthermore, we assessed whether MAP kinase and NF-κB are also involved in mediating CVEC response to a concussive injury (**Figure 3-12 to 3-15**).

3.1 Cellular Morphologies Following Severe Concussive Injury

HA grown on fibronectin-coated coated Bioflex® plate forms a tight, confluent monolayer with little to no gaps between cells. Similarly, hCMEC/D3 also form a tight monolayer on the fibronectin-coated coated Bioflex® plate. In our study, either HA or hCMEC/D3 were subjected to "severe" concussive injury (55% deformation). At 30 minutes following the same degree of stretch, the appearance of HA and hCMEC/D3 monolayers were strikingly different. HA monolayer appears to be retracted with visible gaps between cells. In contrast, hCMEC/D3 monolayer remains fully intact (**Figure 3-1**).

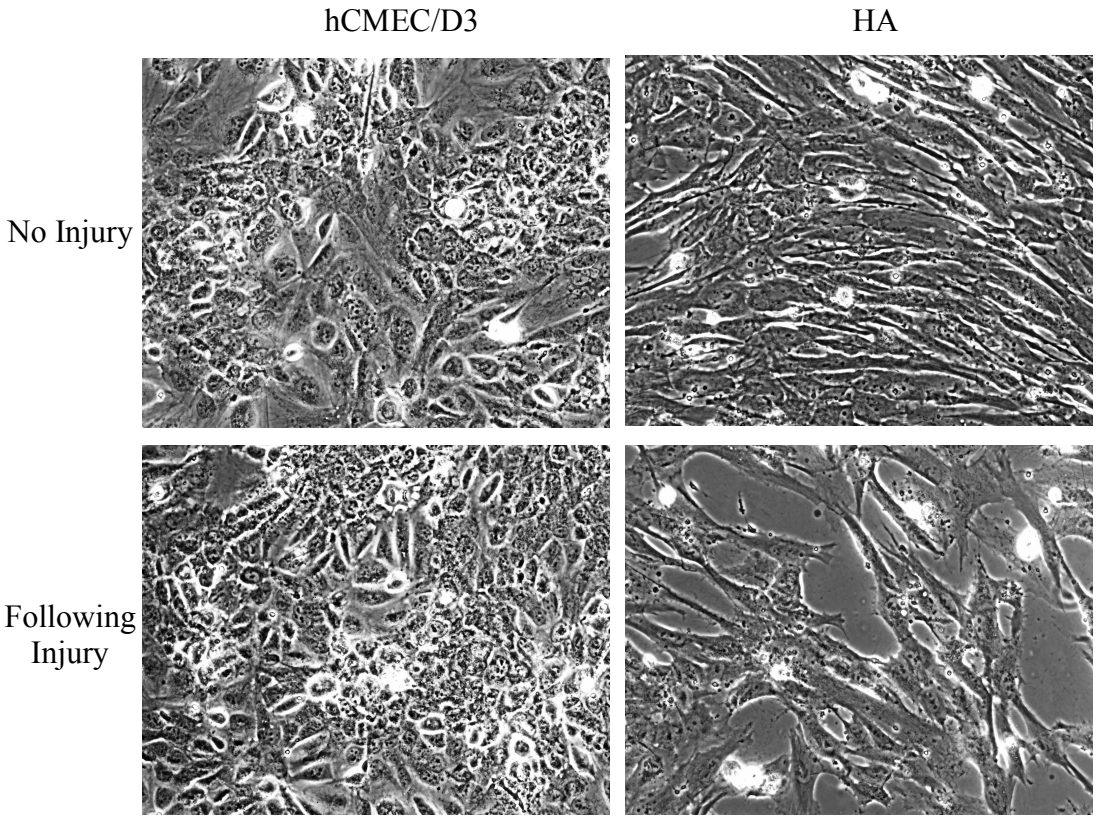

Figure 3-1. Images of hCMEC/D3 and HA Monolayers Following Severe Concussive Injury. Cell monolayer images were captured using light microscopy (50X magnification) at 30 minutes following stretch injury. Top panel depicts uninjured cells for comparisons. No obvious changes are observed in the appearance of injured hCMEC/D3 monolayer compared to uninjured cells. In contrast, concussively injured HA monolayer appears retracted with increased intercellular spaces between astrocytes.

3.2 Quantification of HA Monolayer Retraction

To quantify the level of HA retraction, we compared images of fluorescent-stained HA following injury with uninjured HA monolayer. From a given image, the ImageJ software automatically measures the surface area covered by cells (light area) relative to the dark background (no cells). The percent of surface area occupied by cells were then calculated to provide a quantitative value of monolayer retraction. The lower the area "occupied by cells", the greater the monolayer retraction.

Uninjured HA formed a tightly packed cell monolayer with little spaces between cells (**Figure 3-2a**). This translates to a higher value for the percent of surface covered by cells (i.e. monolayer coverage area). Following a severe concussive injury (55% deformation) HA retract and form large gaps between cells (**Figure 3-2b**). Therefore, cells would occupy less area in a given surface dimension. Our data indicated that a severe concussive injury (55% deformation) to HA results in monolayer retraction, represented by a decrease in the percentage of area covered by stained cells (**Figure 3-2c**; n=4, * indicates $P<0.05$ according to Mann-Whitney Rank Sum Test).

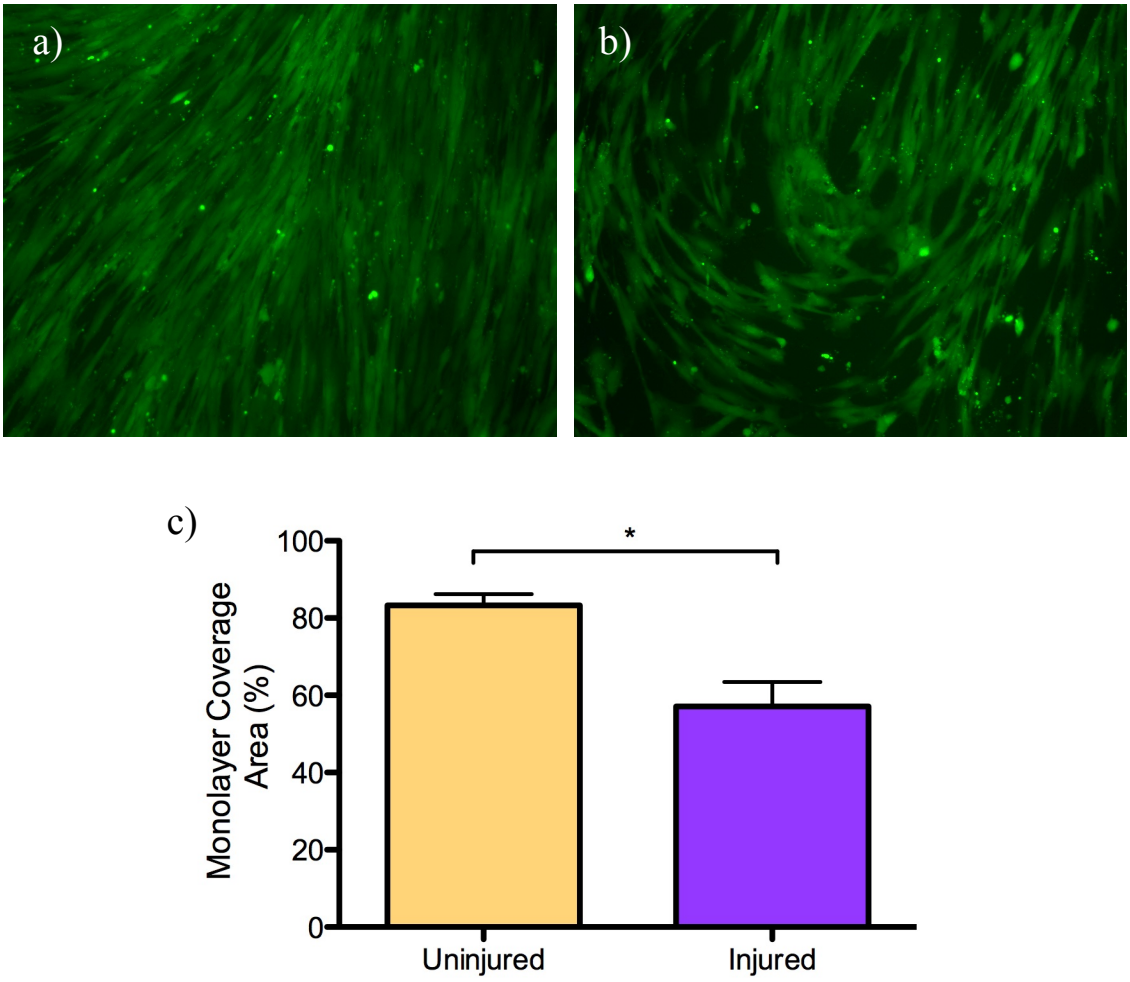

Figure 3-2 HA Monolayer Retraction following a Severe Concussive Injury. HA were pre-incubated with 5, 6-carboxyfluoroscein diacetate (CFDA, 20 μM) and subjected to no injury or severe concussive injury. Fluorescent images of uninjured (a) and injured (b) cell monolayer were captured 30 minutes later. The monolayer retraction was assessed by the quantification of the area covered by the fluorescent-stained HA. (c) Severe concussive injury to HA resulted in monolayer retraction, represented by the decrease in the percentage of area covered by cells (mean±SEM, n=4, * indicates $P < 0.05$ according to Mann-Whitney Rank Sum test). Data were collected from 4 independent experiments, each done in duplicate wells.

3.3 HA Retraction Depends on Severity of Injury

To determine whether HA monolayer retraction varies with the severity of concussive injury, we assessed for monolayer retraction of HA following a mild (20% deformation), moderate (35% deformation) and severe (55% deformation) concussive injury. Quantification of HA monolayer retraction at 30 minutes following injury revealed that HA monolayer integrity is significantly reduced following a severe concussive injury, but not in mild or moderately injured cells (**Figure 3-3**; n=5, * and ** indicates $P < 0.05$ and $P < 0.01$, respectively, according to One Way ANOVA and Tukey's Post Hoc Test). HA monolayer subjected to a severe concussive injury had a significantly lower percentage of monolayer coverage area than moderately injured cells (i.e. more retraction). Thus, HA retraction depends on the degree of injury inflicted upon the cells, and requires a severe concussive injury to induce monolayer retraction.

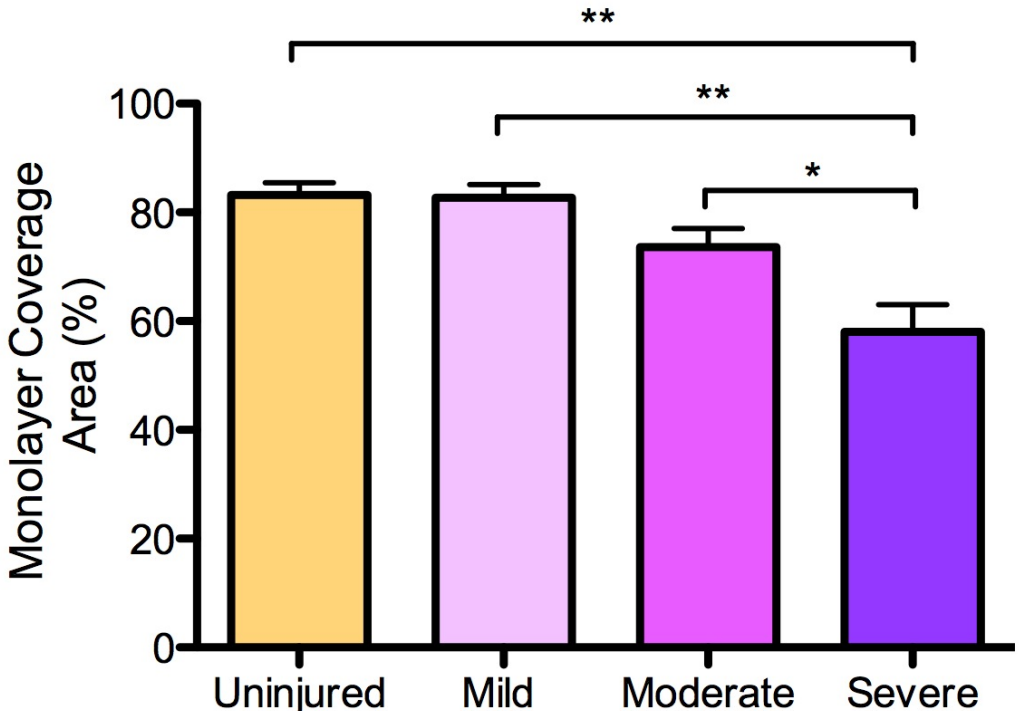

Figure 3-3. HA Monolayer Retraction Following Mild, Moderate and Severe Concussive Injury. HA were pre-incubated with 5, 6-carboxyfluoroscein diacetate (CFDA, 20 μM) and subjected to no injury, mild (20% deformation), moderate (35% deformation) and severe (55% deformation) concussive injury. Fluorescent images of cell monolayers were captured 30 minutes later. The monolayer retraction was assessed by the quantification of the area covered by the fluorescent-stained astrocytes (mean±SEM, n=5, * indicates $P < 0.05$ and ** indicates $P < 0.01$ according to One Way ANOVA and Tukey's Post Hoc Test). Data were collected from 5 independent experiments, each done in duplicate wells.

3.4 HA Retraction is not Due to Cell Detachment

To confirm that the increased gaps between HA following severe concussive injury is due to cellular retraction, and not cellular detachments, we quantified the number of cells in cell media following injury. Our data revealed that there are about 365 and 375 cells per monolayer in the uninjured and injured cell media, respectively (**Figure 3-4**; n=3). There is an average of 335 400 cells in a confluent monolayer per well, so the number of cells detected in the media account for about 0.1% of the total number of cells per well. Therefore, cellular detachment from HA monolayer does not contribute to the appearance of intercellular gaps following severe concussive injury.

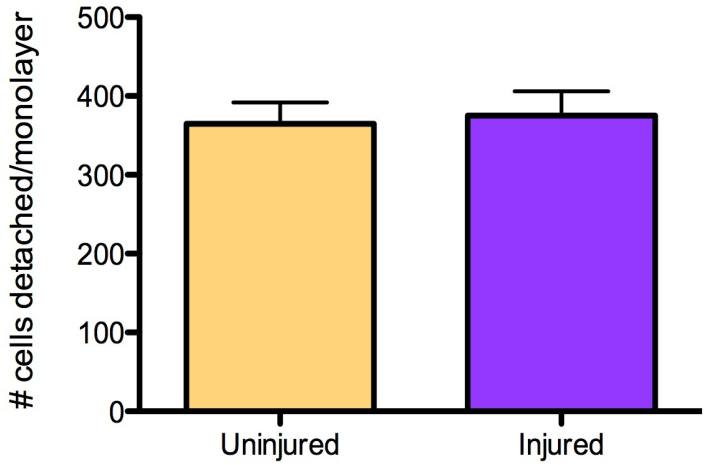

Figure 3-4. HA Detachment from Monolayer Following Severe Concussive Injury. Cell media of uninjured and severely concussed HA monolayer were collected at 30 minutes post-injury. The number of cells in the media was counted using a Haemocytometer and provided the number of cells detached from uninjured and injured HA monolayer (mean ±SEM; n=3). The amounts of detached cells from uninjured and injured monolayer were not significantly different from one another. Data were collected from 3 independent experiments.

3.5 MAP Kinase Activation in HA

To assess for which signaling pathway is involved in concussively-injured cells, we assessed for activations of MAP Kinase by measuring the levels of phosphorylated JNK 1/2, ERK 1/2, and p38 proteins in uninjured and severely injured HA and hCMEC/D3. Detected Western blots of JNK 1/2, ERK 1/2, and p38 were quantified and standardized to GAPDH levels in the samples, presented as the optical density (O.D.) of phospho-JNK 1/2, -ERK 1/2 and -p38 over GAPDH. Representative bands from 3 independent experiments are shown in **Figure 3-5**.

Assessment of phosphorylated JNK 1 and 2 levels indicate that JNK 1/2 are activated in HA at 30 minutes following a severe concussive injury (**Figure 3-6)**. Quantification of JNK 1/2 immunoblots revealed that there was almost a 3-fold increase in the levels of phosphorylated JNK 1/2 in injured HA relative to uninjured cells (**Figure 3-6**; n=6, * indicates $P < 0.05$ according to student t-test). There was also a moderate, however significant increase in the levels of phosphorylated ERK 1 in injured HA relative to uninjured cells (**Figure 3.7**; n=10, * indicates $P < 0.05$), suggesting a concussive injury-induced ERK 1 activation. Levels of phospho-ERK 2 (**Figure 3-7;** n=10) and phospho-p38 (**Figure 3-8;** n=6) were not significantly higher in injured HA relative to uninjured HA, which suggest that ERK 2 and p38 are not activated in HA following a severe concussive injury.

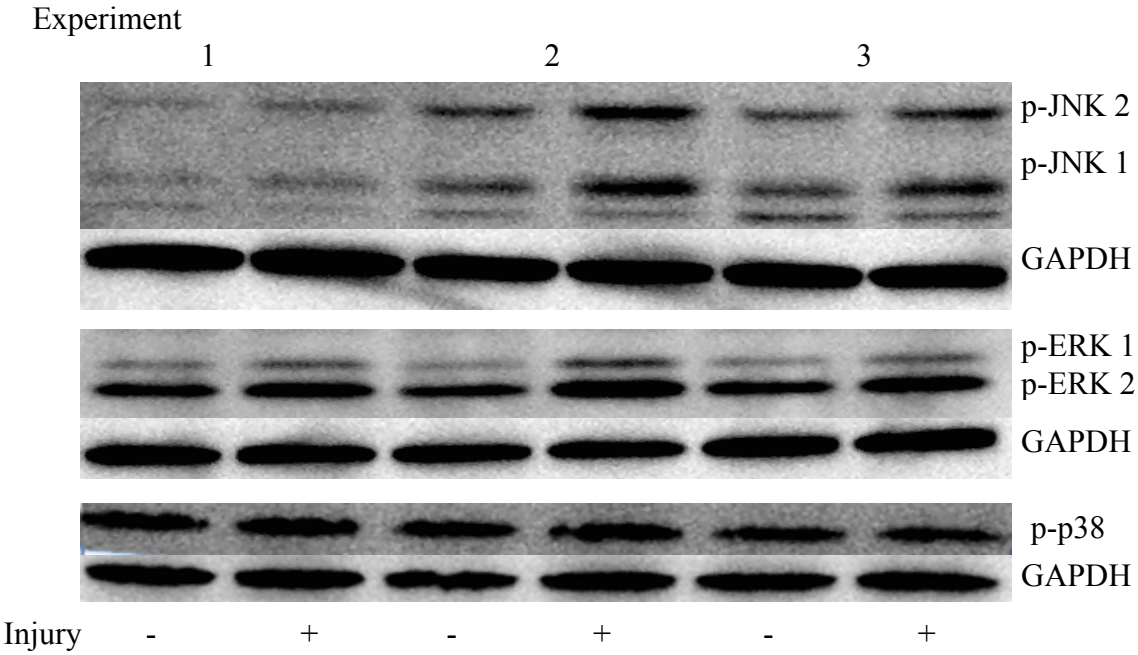

Figure 3-5. MAP Kinase Phosphorylation in HA. Uninjured and severely-injured HA were lysed in 1X SDS sample buffer at 30 minutes post-injury and subsequently subjected to SDS-PAGE. Proteins were transferred by Western blotting onto a PVDF membrane and probed with antibodies against phosphorylated JNK 1/2 (p-JNK 1/2), phosphorylated ERK 1/2 (p-ERK 1/2) or phosphorylated p38 (p-p38). GAPDH served as loading control. Protein bands were visualized by chemiluminescence. Representative immunoblots from 3 independent experiments are shown above.

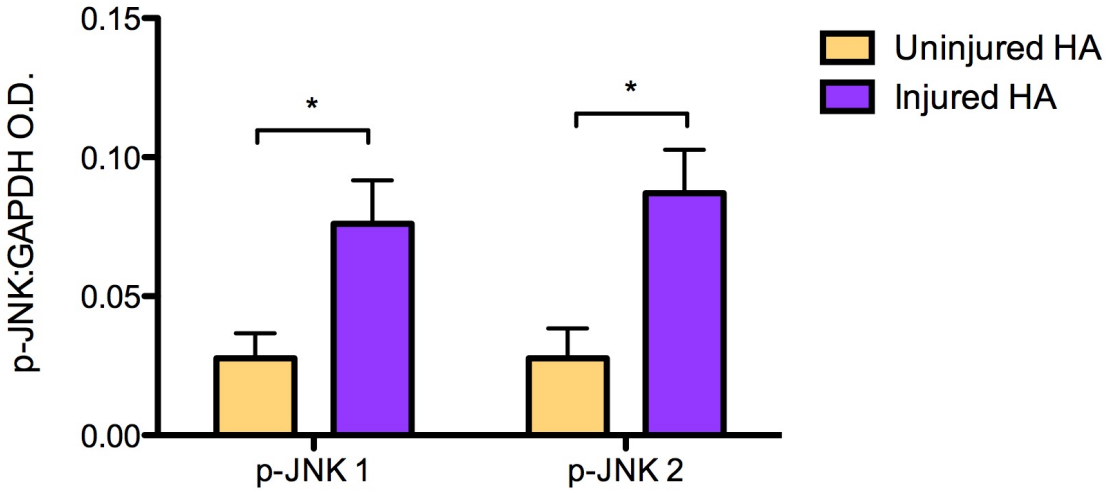

Figure 3-6. Levels of phosphorylated JNK 1/2 in HA Following Severe Concussive Injury. Western blotting was performed to detect levels of phosphorylated JNK 1/2 (p-JNK 1/2) in uninjured and severely concussed HA at 30 minutes post-injury. Protein bands corresponding to p-JNK 1/2 were quantified and standardized to the levels of the loading control protein, GAPDH. Relative levels of p-JNK1/2 are presented as the optical density (O.D.) of p-JNK 1/2 over GAPDH. Levels of p-JNK 1/2 are significantly higher in injured HA compared to uninjured cells (mean±SEM, n=6, * indicates $P < 0.05$ according to student t-test). Data were collected from 6 independent experiments.

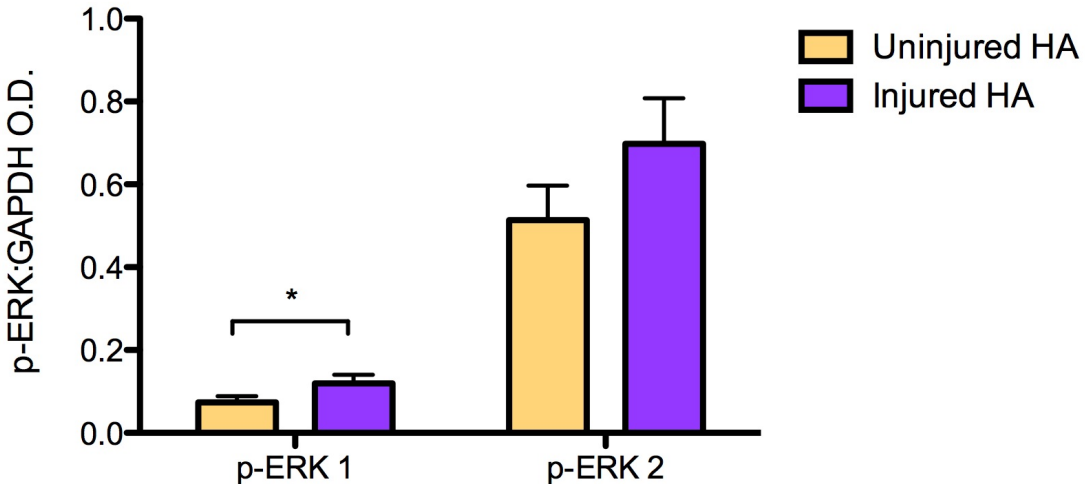

Figure 3-7. Levels of phosphorylated ERK 1/2 in HA Following Severe Concussive Injury. Western blotting was performed to detect levels of phosphorylated ERK 1/2 (p-ERK 1/2) in uninjured and severely concussed HA at 30 minutes post-injury. Protein bands corresponding to p-ERK 1/2 were quantified and standardized to the levels of the loading control protein, GAPDH. Relative levels of p-ERK 1/2 are presented as the optical density (O.D.) of p-ERK 1/2 over GAPDH. There is a significant increase in p-ERK 1 in injured HA relative to uninjured cells (mean±SEM, n=10, * indicates $P < 0.05$ according to Mann-Whitney Rank Sum test). Data were collected from 10 independent experiments.

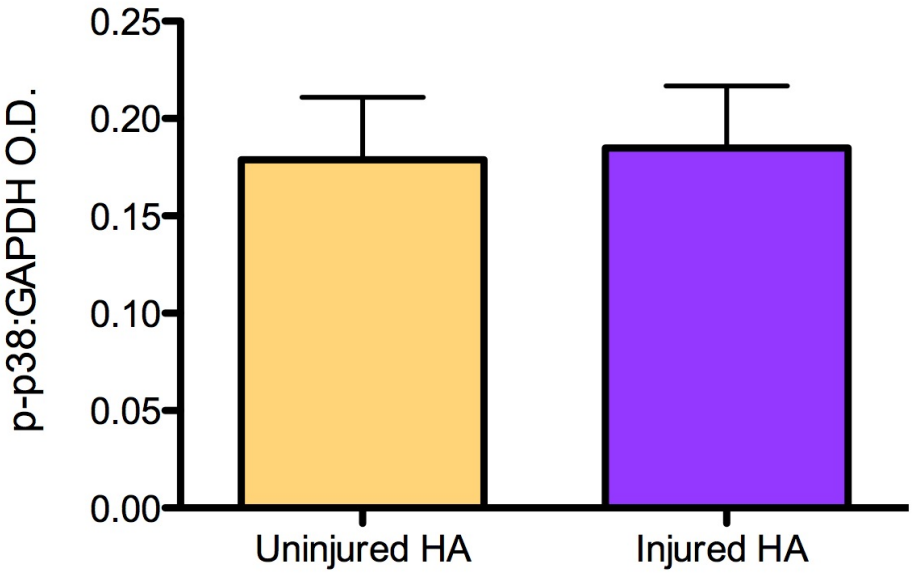

Figure 3-8. Levels of phosphorylated p38 in HA Following Severe Concussive Injury. Western blotting was performed to detect levels of phosphorylated p38 (p-p38) in uninjured and severely concussed HA at 30 minutes post-injury. Protein bands corresponding to p-p38 were quantified and standardized to the levels of the loading control protein, GAPDH. Relative levels of p-p38 are presented as the optical density (O.D.) of p-p38 over GAPDH (mean±SEM, n=6). Data were collected from 6 independent experiments.

3.6 JNK Inhibitors Block HA Retraction Following Severe Concussive Injury

Our findings revealed that severe concussive injury induces an almost 3-fold increase in phosphorylated JNK 1/2, suggesting a JNK 1/2 activation following injury. To assess whether JNK activation is an associated mechanism for mediating HA monolayer retraction following a severe concussive injury, we employed 2 structurally distinct selective JNK inhibitors: SP600125 and SU3327. HA were pre-treated with 25 μM of SP600125 or SU3327 for 10 minutes prior to injury. HA retraction was assessed with CFDA-stained astrocytes, as described above.

Similar to the previous experiments, application of severe concussive injury to HA monolayer resulted in cellular retraction, with respect to percent of surface area covered by cells. However, pre-treatment with JNK inhibitor, SP600125 reduces the extent of retraction such that HA pre-treated with SP600125 had some monolayer retractions following injury compared to uninjured cells, but the cellular retractions were not as severe as those that were injured without SP600125 (**Figure 3-9**; n=6 * and ** indicates $P < 0.05$ or <0.01, respectively, according to One Way ANOVA and Tukey's Post-hoc test). Monolayer retraction of uninjured and injured HA that were both pre-treated with SP600125 were not significantly different.

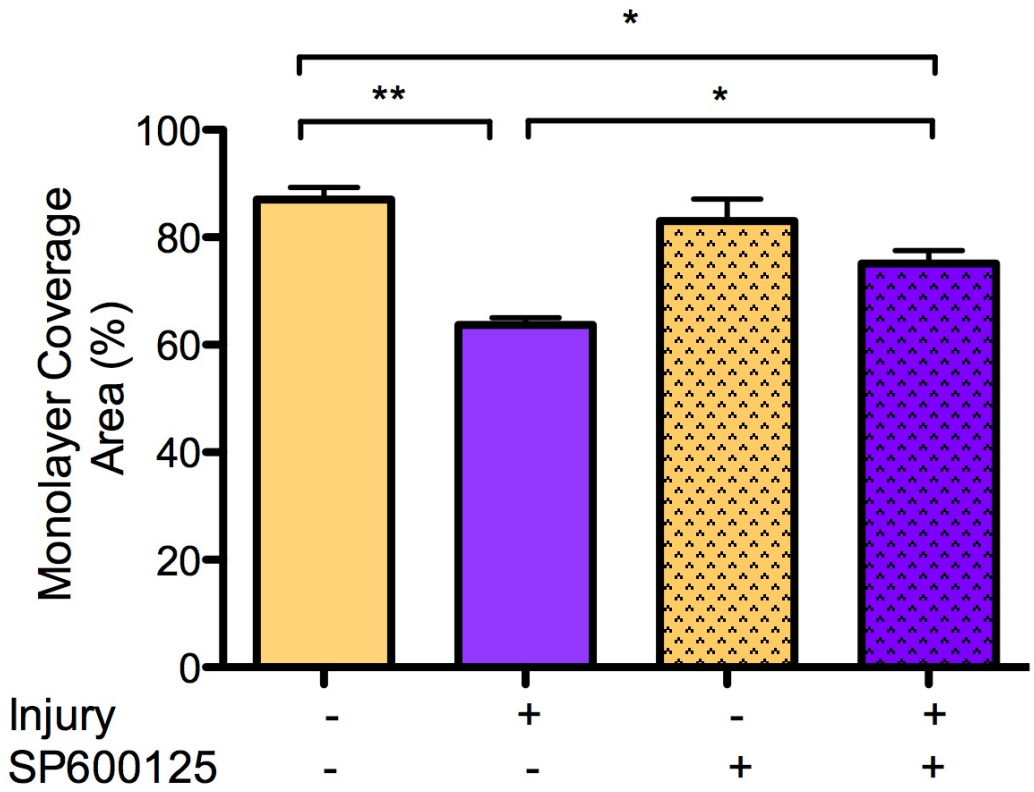

Figure 3-9. HA Monolayer Retraction with SP600125 Pre-treatment. Confluent HA were stained with 5,6-CFDA and pre-treated with 25 μM of SP600125 for 10 minutes prior to a severe concussive injury. Fluorescent images of HA monolayers were captured at 30 minutes following injury, and the monolayer retraction was presented as the percent of surface area covered by cells. In the absence of inhibitors, severe concussive injury induces monolayer retraction. HA pre-treated with SP600125 exhibited less monolayer retraction than the cells injured in the absence of JNK inhibitor (mean±SEM; n=6, * and ** indicates $P < 0.05$ or < 0.01, respectively, according to One Way ANOVA and Tukey's Post-Hoc test). Data were collected from 6 independent experiments, each done in duplicate wells.

To confirm our findings, we employed a second selective JNK inhibitor, SU3327, to assess whether inhibition of JNK 1/2 blocks concussively injured HA monolayer retraction. Again, severe concussive injury induces HA monolayer retraction compared to uninjured cells. HA monolayer pre-treated with SU3327 did not exhibit any significant monolayer retraction relative to uninjured cells, suggesting that inhibiting JNK blocks HA retraction following a severe concussive injury (**Figure 3-10;** n=5, * and ** indicates $P < 0.05$ or < 0.01, respectively, according to One Way ANOVA and Tukey's Post-hoc Test).

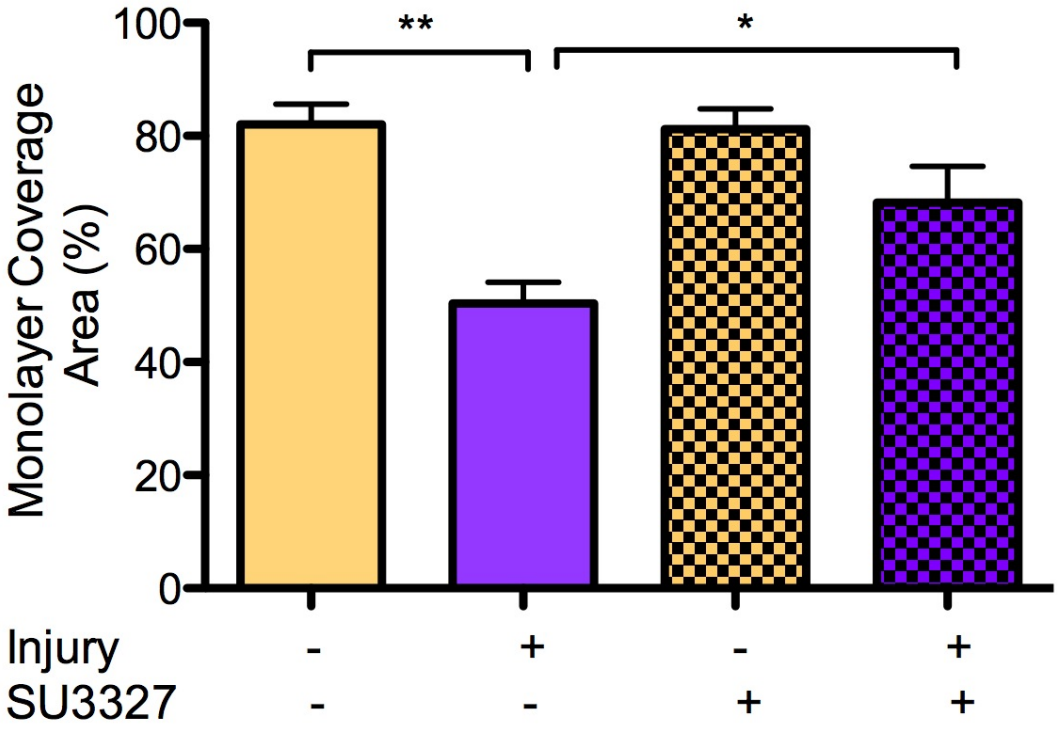

Figure 3-10. HA Monolayer Retraction with SU3327 Pre-Treatment. Confluent HA were stained with 5,6-CFDA and pre-treated with 25 μM of SU3327 for 10 minutes prior to a severe concussive injury. Fluorescent images of HA monolayers were captured at 30 minutes following injury, and monolayer retraction was presented as the percent of surface area covered by HA. In the absence of inhibitors, concussive injury reduced HA monolayer integrity. HA monolayer integrity for cells pre-treated with SU3327 were not significantly lower than uninjured cells, suggesting that JNK inhibition blocks HA monolayer retraction (mean±SEM; n=5, * and ** indicates $P < 0.05$ or < 0.01, respectively, according to One Way ANOVA and Tukey's Post-Hoc Test). Data were collected from 5 independent experiments, each done in duplicates.

3.7 Concussive Injury Up-regulates hCMEC/D3 Pro-adhesive Phenotype

Unlike HA, severe concussive injury (55% deformation) does not induce apparent change in hCMEC/D3 cellular morphology (**Figure 3-1**). Thus we assessed for other aspects of how stretch injury affects CVEC. Animal models of TBI reported PMN accumulations in the brain following trauma, which likely involves the up-regulation of CVEC pro-adhesive phenotype [7, 11, 24, 25]. Therefore, we assessed for PMN adhesive interactions with hCMEC/D3 monolayer under "static" condition after a severe concussive injury. Data from our study revealed that there was an almost 2-fold significantly larger amount of PMN adhering to injured hCMEC/D3 monolayer relative to uninjured cells at 4 hours following injury (**Figure 3-11;** n=6, * indicates $P < 0.05$, according to student t-test).

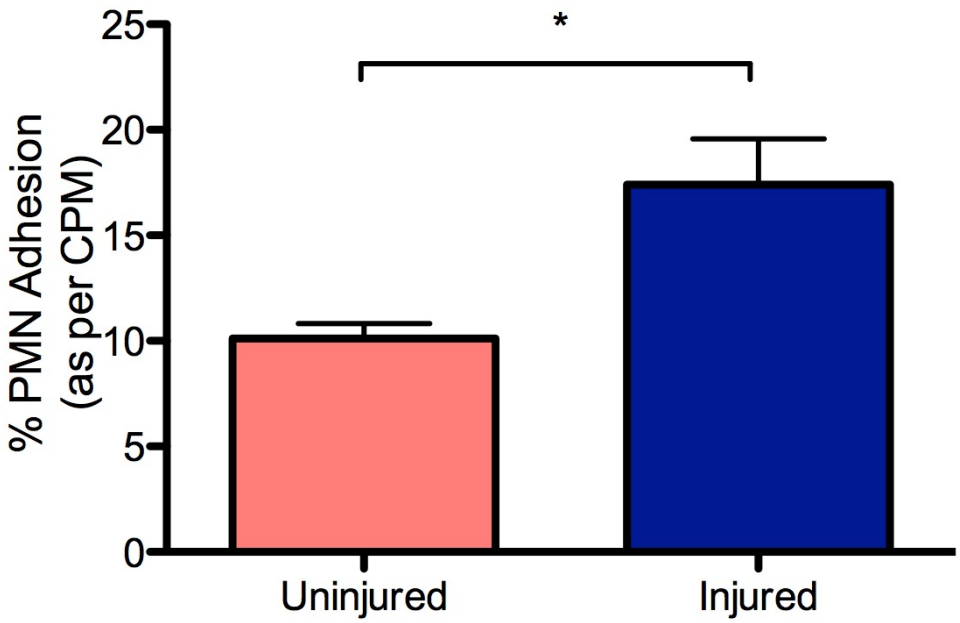

Figure 3-11. PMN Leukocyte Adhesion to Injured hCMEC/D3 Monolayer. ^{51}Cr labeled PMN were added to hCMEC/D3 monolayer (5:1 PMN/hCMEC/D3 ratio) for 30 minutes at 4 hours following injury. Injured hCMEC/D3 monolayer had a significantly higher amount of adhering PMN relative to uninjured cell monolayer (mean±SEM, n=6, * indicates $P < 0.05$ according to student t-test). Data were collected from 6 independent experiments, each done in duplicate wells.

3.8 MAP Kinase Not Activated in Injured hCMEC/D3

Our assessment of PMN adhesion to injured hCMEC/D3 monolayer indicates that a severe concussive injury induces the up-regulation of pro-adhesive phenotype in CVEC. Subsequently, we assessed whether the injury-induced cellular response in hCMEC/D3 is regulated by MAP kinase activation. We measured levels of phospho-JNK 1/2 (p-JNK 1/2), phospho-ERK 1/2 (p-ERK1/2), and phospho-p38 (p-p38) in uninjured and injured hCMEC/D3 at 30 minutes following a severe concussive injury. Similar to the HA experiments, levels of the phosphorylated MAP kinase proteins detected were standardized to GAPDH serving as protein loading control. For a positive assay control, samples of hCMEC/D3 treated with a known MAP kinase inducer (Cytomix; CM: 10 ng/mL TNF-α, IL-1β, and IFN-γ) were loaded in parallel to the uninjured and injured cells. Detected Western blots of ERK 1/2 and p38 were quantified and standardized to GAPDH levels in the samples, presented as the optical density (O.D.) of phospho-ERK 1/2 and -p38 over GAPDH. Representative images from 3 independent experiments are shown in **Figure 3-12.** Bands corresponding to cytomix-treated cells (positive control) appeared darker than other bands, which confirms that MAP kinase activation is detectable in hCMEC/D3 using our current experimental protocol.

Our results indicate that JNK 1/2, ERK 1/2, and p38 are not activated in hCMEC/D3 at 30 minutes following injury. Bands corresponding to p-JNK 1/2 were detected in CM-treated cells, but not in uninjured and stretch-injured cells (**Figure 3-12**). Levels of p-ERK 1/2 (**Figure 3-13;** n=3), and p-38 (**Figure 3-14;** n=3) are not significantly higher in injured hCMEC/D3 compared to uninjured cells. Thus MAP

kinase does not seem to be activated in hCMEC/D3 at 30 minutes following a severe concussive injury.

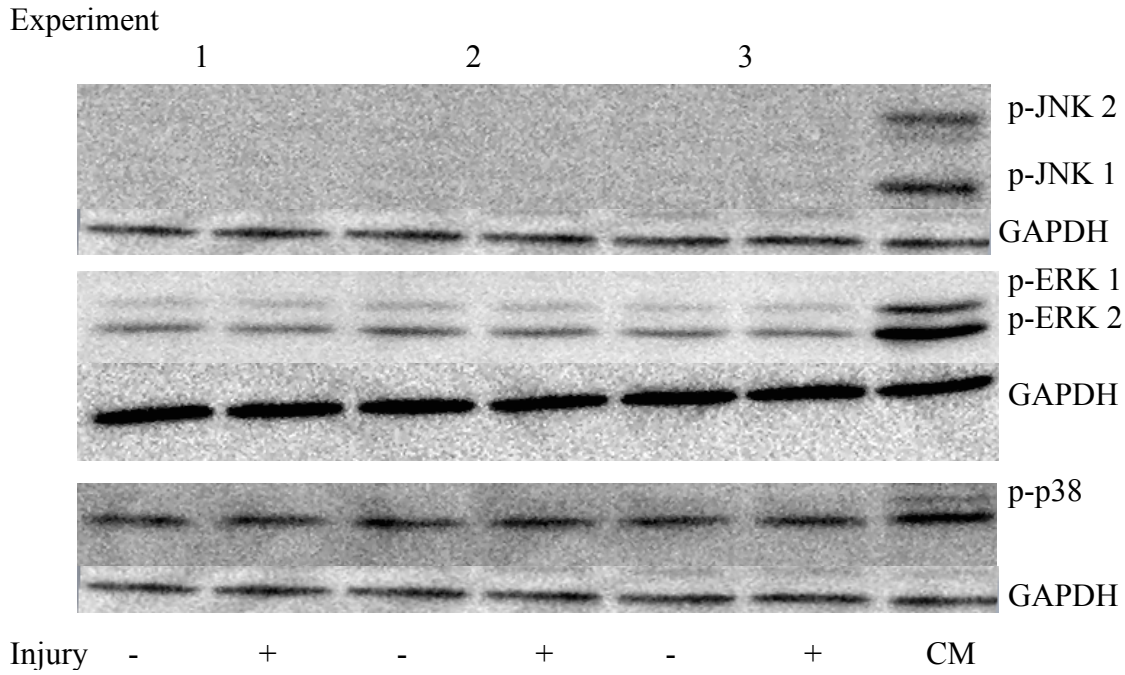

Figure 3-12. MAP Kinase Phosphorylation in hCMEC/D3. Uninjured and injured hCMEC/D3 were lysed in 1X SDS sample buffer at 30 minutes post-injury and subsequently subjected to SDS-PAGE. hCMEC/D3 treated with cytomix (CM; 10 ng/mL TNF-α, IL-1β and IFN-γ) served as a positive control. Proteins were transferred by Western blotting onto a PVDF membrane and probed with antibodies against phosphorylated JNK 1/2 (p-JNK 1/2), phosphorylated ERK 1/2 (p-ERK 1/2) or phosphorylated p38 (p-p38). GAPDH served as loading control. Protein bands were visualized by chemiluminescence. Representative immunoblots from 3 independent experiments are shown above.

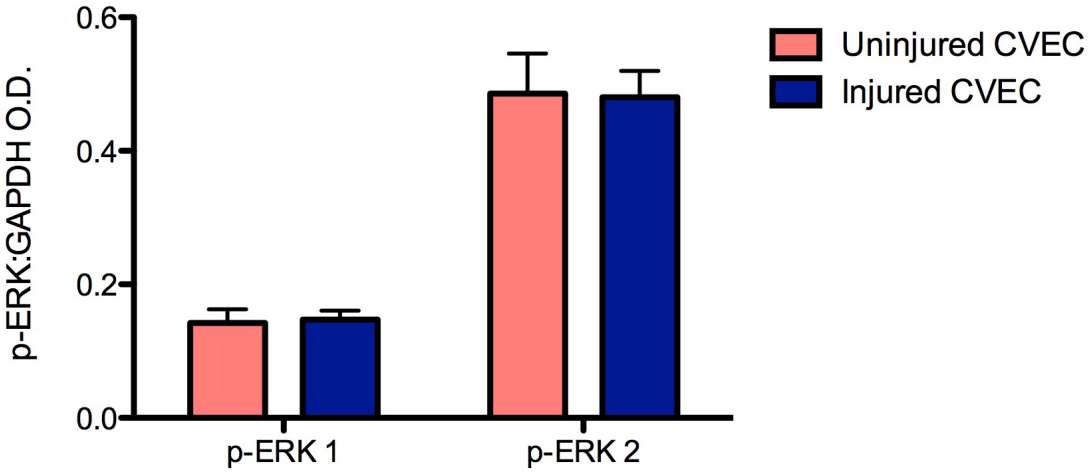

Figure 3-13. Levels of phosphorylated ERK 1/2 in Injured hCMEC/D3. Western blotting was performed to detect levels of phosphorylated ERK 1/2 (p-ERK 1/2) in uninjured and concussed hCMEC/D3 at 30 minutes post-injury. Protein bands corresponding to p-ERK 1/2 were quantified and standardized to the levels of the loading control protein, GAPDH. Relative levels of p-ERK 1/2 are presented as the optical density (O.D.) of p-ERK 1/2 over GAPDH (mean±SEM, n=3). Data were collected from 3 independent experiments.

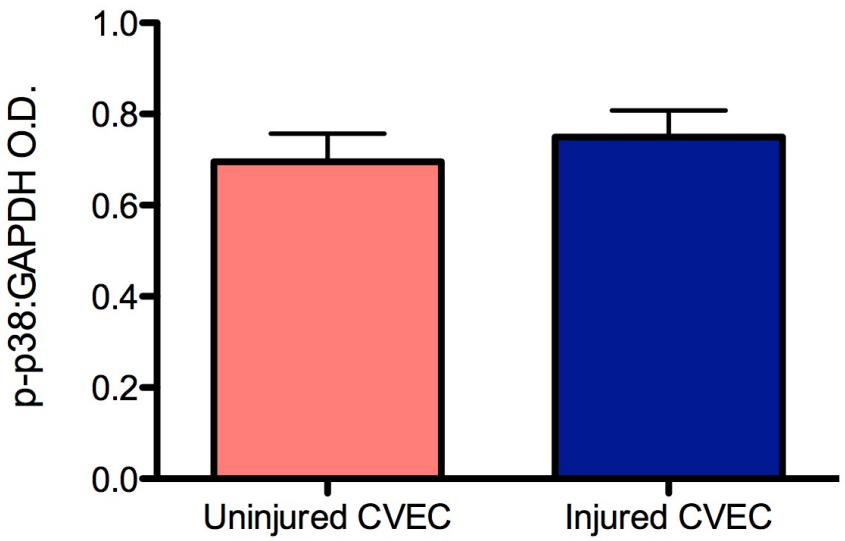

Figure 3-14. Levels of phosphorylated p38 in Injured hCMEC/D3. Western blotting was performed to detect levels of phosphorylated p38 (p-p38) in uninjured and concussed hCMEC/D3 at 30 minutes post-injury. Protein bands corresponding to p-p38 were quantified and standardized to the levels of the loading control protein, GAPDH. Relative levels of p-p38 are presented as the optical density (O.D.) of p-p38 over GAPDH (mean±SEM, n=3). Data were collected from 3 independent experiments.

3.9 Activation of NF-κB was not Detected in Injured hCMEC/D3

To investigate an alternative pathway that may be involved in hCMEC/D3 response to injury with subsequent up-regulation of CVEC pro-adhesive phenotype, we assessed for relative NF-κB activation in hCMEC/D3 using a phospho-NF-κB p65 (Ser536) Sandwich ELISA. Relative NF-κB activation was assessed with respect to the levels of phospho-NF-κB p65 in injured hCMEC/D3 compared to levels found in uninjured cells at 1 hour post-injury. Experiments were conducted according to protocol provided by the kit's manufacturer (see *Methods*). Cellular levels of phospho- NF-κB p65 were presented as the optical density (O.D.) reading at 450 nm.

Results from the phospho-NF-κB p65 ELISA indicated that relative levels of phospho- NF-κB p65 in injured hCMEC/D3 were not significantly higher than levels in uninjured cells (**Figure 3-15;** n=6). This suggests that at 1 hour post-injury, an elevated level of phospho-NF-κB p65 is not involved in hCMEC/D3 following concussive injury.

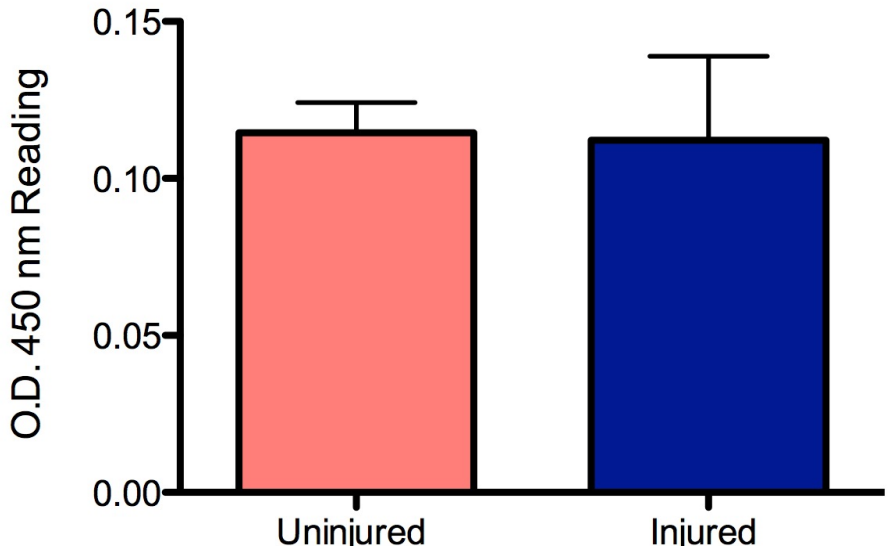

Figure 3-15. NF-κB Activation in hCMEC/D3 Following Severe Concussive Injury. Cellular activation of NF-κB was assessed with respect to phosphorylated-NF-κB p65 (Ser536) using Sandwich ELISA. Uninjured and concussed hCMEC/D3 were collected at 1 hour following injury and tested for phospho-NF-κB p65 using the protocol provided with the ELISA kit. Detected phospho-NF-κB p65 were read at 450 nm and presented as the assay's optical density (O.D.; mean±SEM; n=6). Data were collected from 6 independent experiments.

Chapter 4

4 Discussion

Results from our experiments revealed that a severe concussive injury (55% deformation) induces retraction of the HA monolayer. Mild (20% deformation) and moderate (35% deformation) concussive injury appears to spare trauma-induced HA retraction. Severe concussive injury does not induce HA detachment from monolayer. Concussive injury also induces the activation of JNK 1/2 and ERK 1 in HA at 30 minutes following injury. Our data suggest that JNK 1/2 may be involved in mediating injury-induced HA retraction. Inhibition of JNK in HA reduces HA retraction following severe injury.

In contrast to HA, concussive injury to immortalized CVEC, hCMEC/D3, fails to induce monolayer retraction. Thus, the same degree of injury to HA and hCMEC/D3 caused differential cellular response with respect to cellular morphology. Although there does not seem to be obvious monolayer disruption, concussively injured hCMEC/D3 exhibited an up-regulation of pro-adhesive phenotype. There were more PMN adhering to injured hCMEC/D3 monolayer compared to uninjured cells. MAP kinase JNK 1/2, ERK 1/2, and p38 were not activated in hCMEC/D3 at 30 minutes following injury. Furthermore, NF-κB activation was also not detected in concussively injured hCMEC/D3.

4.1 Severe Concussive Injury Induces HA Retraction

HA grown on a fibronectin-coated culture well form a tightly packed confluent monolayer, with few small gaps between cells. Following a severe concussive injury, there is a change in the appearance of HA monolayer. Injured HA monolayer appears retracted with the presence of large gaps or spaces between cells. In order to quantify this phenomenon, we developed an assay to assess cell monolayer retraction. Confluent HA were pre-stained with whole-cell fluorescent dye, 5, 6-carboxyfluoroscein diacetate (CFDA), that allows for real-time fluorescent imaging of live HA cell culture. The fluorescent stain provided a greater contrast between cells and the background (culture membrane). Images of uninjured and injured CFDA-stained HA monolayer were captured by fluorescent microscopy, and the percent of surface area covered in cells in each picture were quantified using the ImageJ software. This provided a quantified value of monolayer retraction (with respect to the percent of monolayer coverage).

The assessment of HA monolayer integrity revealed that a severe concussive injury to primary human astrocytes result in an increase in monolayer retraction. Despite the dramatic change in cell morphology, severely injured astrocytes remained adherent to culture membrane after injury; we detected negligible amounts of detached cells in culture media following injury. This suggests that membrane area that is absent of cells following concussive injury to HA is likely due to a change in HA morphology, as opposed to a mere detachment of cells from the membrane, for leaving gaps of space throughout the monolayer.

Furthermore, we investigated whether HA monolayer retraction also occurs following a less severe injury. Therefore, in addition to severe injury, we assessed the

monolayer integrity of HA monolayer following a mild and moderate concussive injury. Our data revealed that cellular retraction does not occur following a mild and moderate concussive injury. Therefore, HA retraction seems dependent on the severity of the injury and occurs only following severe concussive injury. Results from our study correlates with earlier works that employed cultured primary rat astrocytes to model TBI *in vitro.* Similar to the *human* primary astrocytes used in this study, rat astrocytes exhibited cellular retraction following a severe concussive injury (55% stretch) [9, 54]. Although retracted, rat astrocytes also appeared to remain adherent to the culture membrane, as no significant cellular detachment occurred following injury [9, 54].

4.2 MAP Kinase Activation in Injured HA

To assess for a potential mechanism mediating the change in HA morphology following a severe concussive injury, we assessed for MAP kinase activation in HA following injury. Activation of the MAP kinase pathways involves the phosphorylation of their subunits, which allows for rapid signal transduction in response to stress or injury [41]. Results from our study indicated that at 30 minutes following injury, JNK 1/2, as well as ERK 1 is activated in HA. In our experimental conditions, p38 does not seem to be activated following severe stretch injury. These findings are in contrast to a study using *in vitro* and *in vivo* rat models of TBI that noted the activation of ERK 1/2 and p38, whereas JNK phosphorylation remain unchanged [26, 37]. Variations between our study and what has previously been reported may be due to the different types of

trauma model used – we employed a stretch injury to mimic a biaxial force TBI, which may induce a different cellular response than if other TBI models were used (i.e. cortical impact and mechanical scratch injuries) [40]. Furthermore, our study employs the use of primary *human* astrocytes rather than rat cells. Thus specific induction of MAP kinase may be dependent on which cell models were used (i.e. humans versus animal).

Based on the data obtained in our study, there are notable activations of JNK 1/2 in injured HA, which coincides with the appearance of monolayer retraction. JNK is activated by many factors, including environmental stress, ischemic reperfusion injury, genotoxins, pro-inflammatory cytokines, and mechanical stress [41]. The JNK signaling pathway governs many cellular functions, including various gene transcriptions, apoptosis and cell morphology [41]. MAP kinase has been reported to mediate astrocyte swelling following TBI [33]. The use of various inhibitors, including a JNK inhibitor SP600125, prior to injury significantly reduces rat astrocyte swelling following injury. Furthermore, the JNK pathway has been implicated in the maintenance of cytoskeletal structure in cells of the CNS [55]. Stability of the microtubules in a cell plays a pivotal role in the maintenance of cell shape, and JNK have been reported to be involved in regulating microtubule dynamics in neuronal cells [55]. As such, we assessed whether HA monolayer retraction following a severe concussive injury is mediated by JNK 1/2 activation.

4.3 HA Retraction Mediated by JNK

To address the role of JNK 1/2 activation in HA retraction following a severe concussive injury, we employed 2 commercially available selective JNK inhibitors, SP600125 and SU3327. These 2 inhibitors selectively inhibit JNK using 2 different mechanisms. SP600125 is a reversible, competitive JNK 1/2/3 inhibitor that interferes with ATP binding to the JNK subunits [51]. SU3327 is a more recently developed selective JNK inhibitor, which prevents the protein-protein interactions between JNK and JNK Interacting Protein (JIP) [53]. In the absence of JNK inhibitors, concussive injury to HA induced monolayer retraction. Pre-treatment of with JNK inhibitors prior to injury reduced the extent of HA retraction following severe concussion. Similar results were obtained using the two different JNK inhibitors, which strengthen the suggestion that injury-induced change in HA morphology following a severe concussive injury (i.e. monolayer retraction) is likely mediated by the JNK signaling pathway.

The exact mechanism of how JNK mediates HA retraction and alter cellular morphology following injury is not yet known. JNK may alter cellular morphology directly by interacting with cytoskeleton-associated proteins, or indirectly by mediating the activity of another protein that leads to a downstream change in cellular cytoskeleton dynamics [44, 55]. In neurons, JNK 1 phosphorylates microtubule-associated proteins, altering microtubule dynamics and in turn, cell morphology [55]. MAP kinase regulation of microtubule-associated proteins has also been implicated in regulating microtubule cytoskeletons in non-neuron cells during various cellular events [55]. JNK may also regulate cell morphology through its interaction with other

signaling molecules. For example, ubiquitous protein kinase CK2 regulates the phosphorylation of actin and myosin light chain proteins in astrocytes [44]. Activation of CK2, which may be mediated by MAP kinase activities, alters the phosphorylation of microtubule-associated proteins and induces cell contractions [44]. Changes to actin filaments (i.e. actin filament assembly/disassembly) may be accompanied by rearrangement of integrin-mediated focal adhesion to facilitate in modifications of cell morphology (i.e. cell retraction) in astrocytes [45, 46]. Further investigations must be conducted to determine the upstream and downstream mechanisms in JNK-mediated HA retraction following severe concussive injury.

4.4 Severe Concussive Injury Fails to Induce hCMEC/D3 Retraction

Human immortalized CVEC, hCMEC/D3 grown on a fibronectin-coated culture well form a dense, confluent cell monolayer with no gaps between cells. Morphologically, this mimics CVEC *in vivo*, which form a tight monolayer on the luminal side of the microvasculature that restricts the movements of substances across the blood vessel [47]. Following a severe concussive injury with a 55% membrane deformation, hCMEC/D3 monolayer appears intact and does not exhibit any sign of retraction. This is in contrast to HA monolayer, which appears dramatically retracted following the same degree of injury to hCMEC/D3. This suggests that HA are more severely affected by concussive injury than hCMEC/D3. One caveat in our study is the use of immortalized CVEC, which potentially may explain why hCMEC/D3 are less

sensitive to monolayer changes than the primary astrocytes. However, a study that employed the use of primary rabbit and bovine endothelial cells found that endothelial cells were much more resistant to a stretch injury and require a greater degree of injury to produce the same extent of injury than astrocytes [54]. Endothelial cells also appeared to recover more rapidly following injury than astrocytes and neural glial cells [54]. Therefore, it is more likely that the degree of injury applied to hCMEC/D3 in our experimental approach simply were not enough to induce a physical disruption of CVEC monolayer. Although the concussively injured hCMEC/D3 do not appear to be morphologically altered, we assessed for a cellular response to injury with respect to PMN adhesion to injured CVEC monolayer.

4.5 Severe Concussive Injury Up-regulates hCMEC/D3 Pro-adhesive Phenotype

In a healthy individual, there are little interactions between CVEC lining the microvasculature and circulating immune cells [3]. As a result, migration across the endothelium is restricted by the BBB and very few immune cells are found in the CNS [3]. CVEC play a role in mediating inflammation in CNS with respect to its interactions with circulating immune cells such as PMN [3]. Under a pathological condition, there may be an up-regulation of endothelial cell pro-adhesive phenotype marked by induced expression of surface adhesion molecules [3]. As more PMN adhere to CVEC, there is a greater opportunity for PMN to migrate across the microvasculature and accumulate in the brain parenchyma.

To address the potential role of CVEC in facilitating the accumulation of PMN following a TBI in humans, we assessed whether there is up-regulation of pro-adhesive phenotype in hCMEC/D3 following a severe concussive injury. Using a radioactive labeled PMN, we observed increase PMN adhering to injured hCMEC/D3 monolayer relative to uninjured cell monolayer. Thus a severe concussive injury induces pro-adhesive phenotype. This is likely due to increased expression of adhesion molecules, such as E-selectin, intercellular adhesion molecules (ICAM-1, ICAM-2) or vascular cell adhesion molecule (VCAM-1), on the surface of endothelial cells that can interact with selectin-receptors and integrins (e.g. β2 integrins) expressed on the surface of PMN [11, 28]. The exact signaling pathways involved in the up-regulation of CVEC pro-adhesive phenotype following a mechanical injury are not yet known. In this study, we assessed the potential involvement of MAP kinase and NF-κB in hCMEC/D3 following injury.

4.6 Activation of MAP Kinase and NF-κB were not Detected in Injured hCMEC/D3

Levels of phosphorylated ERK 1/2, JNK 1/2 and p38 were assessed in uninjured and injured hCMEC/D3 to assess for MAP kinase activation. Results obtained from our experiments revealed that ERK 1/2, JNK 1/2 and p38 are not activated in concussively injured hCMEC/D3. This is in contrast to HA, which exhibited activation of ERK 1 and JNK 1/2 following injury. Typically, MAP kinase activation occur rapidly following an insult (i.e. within minutes), therefore MAP kinase activation was assessed at 30 minutes following injury. However, if MAP kinase activation occurs later in injured

hCMEC/D3, it would not be detected with our current experimental approach. It is more likely that another signaling pathway is involved in mediating injury-induced hCMEC/D3 response.

One of the major signaling pathways involved in a cellular response to stress is the transcription factor, NF-κB [38]. NF-κB is activated by various pathogenic stimulants and plays a key role in regulating the inflammatory process [38]. Activated NF-κB has been implicated in up-regulating the transcription of surface adhesion molecules in endothelial cells [28]. In our study, relative NF-κB activation in injured hCMEC/D3 compared to uninjured cells were measured at 1 hour following injury, with respect to phosphorylated NF-κB p65 (Ser 536). However, under our experimental condition, we failed to detect elevated levels of phosphorylated NF-κB p65 in injured hCMEC/D3. The activity of the NF-κB pathway is complex and our study was limited to assessing only one measurement of NF-κB activation. It is possible that trauma-induced hCMEC/D3 response is not via an increase in phosphorylation of NF-κB p65 (Ser 536). Further studies must be conducted to confirm whether NF-κB plays a role in hCMEC/D3 response to a traumatic injury. Up-regulation of NF-κB and the subsequent genes translated upon its activation depend on the formation of subunit homodimers or heterodimers and whether they are translocated to the nucleus [38]. Furthermore, NF-κB subunits may also interact with other signaling pathways, such as AP-1 or MAP kinases, in mediating a cellular response following injury [42].

4.7 Clinical Relevance

Results of our study revealed that a severe concussive injury (i.e. TBI) induces astrocyte retraction. ***In vivo,*** **astrocyte retraction may translate to a loss in the intimate cell-cell contact between perivascular astrocyte endfeet and CVEC, as well as the enlargement of perivascular space. Uncoupling of astrocyte-endothelial cell units may result in the loss of communications between neurons and the BBB** [13]. This may impair the astrocytes from regulating capillary vasodilation/ vasoconstriction for a proper hyperemia. As a result, increased neuronal activity may not be accompanied with the proper change in local blood flow to match the metabolic demand [19]. Imbalanced energy supply to the brain may lead to greater damage to the brain tissue and further complicate a TBI.

Our data revealed that a severe concussive injury alone is not enough to induce CVEC monolayer disruption in an isolated system. It is possible that dysfunction to the cerebral endothelium is secondary to trauma, rather than from the initial mechanical injury from the traumatic impact itself. Post-traumatic breakdown of the BBB (with respect of the CVEC) may be mediated by astrocytes. As mentioned above, uncoupling of astrocyte endfeet from endothelial cells may prevent astrocytes from inducing a tight cerebrovascular endothelium [13]. As the capillaries become “leaky”, components of the circulation are no longer restricted in the vasculature and can accumulate in the brain parenchyma [3, 14]. Movements of plasma proteins, ions, and water into the CNS lead to the formation of vasogenic edema, or brain swelling [16]. Indeed, clinical evaluations have reported that diffused brain swelling (DBS) is a common complication following a TBI [21, 23]. Post-mortem examinations of TBI brain victims revealed that

brains with moderate edema had enlarged perivascular space and distended astrocyte processes [21]. Individuals with severe edema exhibited the absence of perivascular astrocyte end-feet surrounding the microvessels and large perivascular space beyond the basement membrane of the cerebral vasculature [21]. Thus the integrity of the support offered by astrocytic endfeet surrounding the cerebral blood vessels seem to correlate with the formation of post-traumatic edema.

Although the concussive injury itself does not appear to induce cerebral endothelium dysfunction, we assessed for another aspect in which a concussive injury may alter CVECs. TBI can elicit an inflammatory response that may worsen neural injuries [7, 11]. Rat models of TBI revealed accumulation of PMN in intracranial space within hours following injury [24, 25]. In our *in vitro* human TBI model, we observed increased PMN adhesion to injured hCMEC/D3 monolayer. Up-regulation of CVEC pro-adhesive phenotype (i.e. increased CVEC-PMN interactions) can facilitate the migration of PMN across the endothelium [7]. However, the mechanisms involved in the up-regulation of endothelial cell pro-adhesive phenotype in hCMEC/D3 following concussive injury and its implications in the development of TBI pathology is yet to be explained and require further investigations.

4.8 Limitations and Future Directions

Our study employed the use of Cell Injury Controller II to model a TBI *in vitro*. This machine induces a uniform, biaxial stretch injury to a cell monolayer grown on a flexible support to mimic an acceleration/deceleration-type of traumatic injury [9]. In

an actual trauma, brain tissues typically experience multiple forms of injuries as opposed to only a single “traumatic blow”. Depending on the type and magnitude of the TBI, different parts of the brain may experience different injuries. Although the mechanical injury used in our experimental condition may represent a simplified model of TBI, the Cell Injury Controller II produces a well-controlled, repeatable injury. The homogeneity of injury in the experiments reduces the technical variability that may arise in our experimental assays.

To assess how a mechanical trauma affects the BBB, we employed the use of primary human astrocytes, HA, and immortalized CVEC, hCMEC/D3. Due to a limited availability of primary human cerebrovascular endothelial cells, we used well-characterized immortalized cell line, hCMEC/D3. Although there are concerns that immortalized cells may differ from its primary counterpart, studies have shown that hCMEC/D3 maintain the expression of key BBB phenotypes, such as the formation of intercellular tight junctions and expressions of surface adhesion molecules [47, 48]. Furthermore, our study assessed astrocytes and endothelial cells in a separate culture. *In vivo*, astrocytes and endothelial cells are found in close proximity and induce BBB-specific phenotypes in one another [15]. As cells are grown and injured separately, we are limited from observing how astrocytes and endothelial cells affect one another. However, separate assessment of each component of the BBB is useful to determine specific astrocyte and endothelial cell response following trauma. In addition, our studies strictly employed the use of human-derived tissues. Therefore, results of this study are highly translational for further understanding of TBI pathology in humans.

Lastly, our experiments were done entirely *in vitro.* In contrast, TBIs *in vivo* are highly heterogeneous and may invoke complex secondary complications beyond the initial trauma, including hypoxia/ischemia, metabolic imbalance, and inflammation [2, 10]. Such complex conditions were not replicated in our experimental approach. Secondary insults associated with TBI may further complicate the cellular response post-injury and requires further investigations.

In future studies, astrocyte and CVEC response to a concussive injury *in vitro* should be assessed in co-culture to further address how injured cells affect one another. Isolated astrocytes exhibited trauma-induced cellular retraction. It would be valuable to assess whether a similar phenomenon occurs in a co-cultured system and how CVEC respond to astrocyte retraction. For instance, we can assess CVEC monolayer permeability using a Texas Red Dextran assay to determine the "tightness" of CVEC monolayer following concussive injury and astrocyte retraction [56]. As CVEC monolayer permeability increases, more Texas Red Dextran would go through the cells. Furthermore, it would be interesting to assess whether trauma-induced cellular injury and dysfunction is worsened in a co-cultured system. Astrocytes and CVEC release factors, such as bradykinin and IL-6, in response to stress and injury, which may induce a greater cellular response in one another [13]. Whether such response is protective or detrimental to further injuries must be determined. For further investigations, animal models may also be employed to assess whether trauma-induced astrocyte process retraction occurs *in vivo*. Results from our study suggest that MAP kinase is involved in mediating astrocyte retraction following injury, and selective MAP kinase inhibitor reduced trauma-induced retraction. If similar results were to be found in an animal

model, we can determine whether minimizing astrocyte endfeet retractions can reduce secondary TBI complications (i.e. dysfunctional cerebral blood flow regulation, brain swelling) and improve the long-term outcomes of TBI.

Results from our study revealed that a severe concussive injury induces JNK-mediated astrocyte retractions. However, we have yet to fully explain exactly how JNK regulates astrocyte morphology. Upstream of JNK activation in astrocytes following injury likely involves ATP/purinergic receptors, which has been implicated in mediating cellular response following stretch injury in rat astrocytes [37]. Effects of JNK on astrocyte morphology must also be further investigated. Following severe injury, JNK may induce the activation of other signaling molecules, such as CK2, which regulates cellular actin-tubulin cytoskeleton network [44]. JNK can also directly affect cellular morphology by phosphorylating microtubule-associated proteins that maintains the cytoskeleton stability in cells [55].

Under our experimental conditions, severe injury alone fails to induce CVEC monolayer disruption. However, CVEC pro-adhesive phenotype was up-regulated following injury, as increased PMN adhesion to injured cells were observed. We have yet to determine which surface adhesion molecules are expressed in injured CVEC and which signaling pathways are involved in mediating the cellular response. Increased expression of surface adhesion molecules E-Selectin, VCAM and ICAM may be determined at a transcriptional level (with real-time polymerase chain reaction; RT-PCR) or at a protein-level (with Western Blotting). Although we failed to detect NF-κB activation in injured hCMEC/D3 with respect to elevated cellular phospho-p65 levels,

we must confirm our finding using other means of measuring NF-κB activation (i.e. levels of I-κB degradation, p50 and p65 nuclear translocation) [39].

Lastly, we observed that treatments with selective JNK inhibitors reduced the severity of astrocyte retraction. With further investigations, this can lead to a potential therapeutic method for reducing the development of complication and improve the long-term outcome of TBI.

References

1. Shlosberg, D., Benifla, M., Kaufer, D., and Friedman, A. (2010). Blood-brain barrier breakdown as a therapeutic target in traumatic brain injury. *Nat. R ev. Neurol.* **6**:393-403.

2. Hiu Lam, W. and Mackersie, A. (1999). Paediatric head injury: incidence, aetiology and management. *Pediatr. Anesth.* **9**:377-385.

3. De Vries, H.E., Kuiper, J., De Boer, A.G., Van Berkel, T.J.C., and Breime, D.D. (1997). The Blood-Brain Barrier in Neuroinflammatory Diseases. *Pharmacol. Rev.* **49**:143-155.

4. Faul, M., Xu, L., Wald, M.M., and Coronado, V.G. (2010). Traumatic Brain Injury in the United States: Emergency Department Visits, Hospitalizations and Deaths 2002-2006. *Centers for Disease Control and Prevention, National Center for Injury Prevention and Control.* Atlanta (GA).

5. Bauer, R. and Fritz, H. (2004). Pathophysiology of traumatic injury in the developing brain: an introduction and short update. *Exp. Toxicol. Pathol.* **56**:65-73.

6. Ducrocq, S., Meyer, P.G., Orliaguet, G.A., Blanot, S., Laurent-Vannier, A., Renier, D., Carli, P.A. (2006). Epidemiology and early predictive factors of mortality and outcome in children with traumatic severe brain injury: Experience of a French pediatric trauma center. *Pediatr. Crit. Care Me.* **7**:461-467.

7. Schmidt, O.I., Heyde, C.E., Ertel, W., and Stahel, P.F. (2005). Closed head injury – an inflammatory disease? *Brain Res. Rev.* **48**:388-399.

8. Saatman, K.E., Duhaime, A., Bullock, R., Maas, A.I.R., Valadka, A., Manley, G.T. (2008). Classification of Traumatic Brain Injury for Targeted Therapies. *J. Neurotraum.* **25**:719-738.

9. Ellis E.F., McKinney, J.S., Willoughby, K.A., Liang, S., and Povlishock J.T. (1995). A New Model for Rapid Stretch-Induced Injury of Cells in Culture: Characterization of the Model Using Astrocytes. *J. Neurotraum.* **12**:325-339.

10. Pascucci, R.C. (1988). Head trauma in the child. *Intens. Care Med.* **14**:185-195.

11. Lenz, A., Franklin, G.A., and Cheadle, W.G. (2007). Systemic inflammation after trauma. *Injury* **38**:1336-1345.

12. Marmarou, A. (2004). The pathophysiology of brain edema and elevated intracranial pressure. *Clev. Clin. J. Med.* **71**:S6-8.

13. Abbott N.J., Rönnbäck, L., and Hansson, E. (2006). Astrocyte-endothelial interactions at the blood-brain barrier. *Nat. Rev. Neurosci.* **7**:41-53.

14. Abbott, N.J., Patabendige, A.A.K., Dolman, D.E.M., Yusof, S.R., and Begley, D.J. (2010). Structure and function of the blood-brain barrier. *Neurobiol. Dis.* **37**:13-25.

15. Wang, D.D. and Bordey, A. (2008). The Astrocyte Odyssey. *Prog. Neurobiol.* **86**: 342-367.

16. Bradbury, M.W. (1985). The blood-brain barrier. Transport across the cerebral endothelium. *Circ. Res.* **57**:213-222.

17. Mathiisen, T.M., Lehre, K.P., Danbolt, N.C., and Ottersen, O.P. (2010). The Perivascular Astroglial Sheath Provides a Complete Covering of the Brain Microvessels: An Electron Microscopic 3D Reconstruction. *Glia* **58**:1094-1103.

18. Janzer, R.C. and Raff, M.C. (1987). Astrocytes induce blood-brain barrier properties in endothelial cells. *Nature* **325**:253-257.

19. Lok, J., Gupta, P., Guo, S., Kim, W.J., Whalen, M.J., van Leyen, K., and Lo, E.H. (2007). Cell-cell Signalling in the Neurovascular Unit. *Neurochem. Res.* **32**:2032-2045.

20. Tanako, T., Tian, G., Peng, W., Lou, N., Libionka, W., Han, X., and Nedergaard, M. (2006). Astrocyte-mediated control of cerebral blood flow. *Nat. Neurosci.* **9**:260-267.

21. Castejón, O.J. (1998). Morphological astrocytic changes in complicated human brain trauma. A light and electron microscopic study. *Brain Injury* **12**:409-427.

22. Inglese, M., Bomsztyk, E., Gonen, O., Mannon, L.J., Grossman, R.I., and Rusinek, H. (2005). Dilated Perivascular Spaces, Hallmarks of Mild Traumatic Brain Injury. *Am. J. Neuroradiol.* **26**:719-724.

23. Ransohoff, R.M., Kivisäkk, P., and Kidd, G. (2003). Three or More Routes for Leukocyte Migration into the Central Nervous System. *Nat. Rev. Immunol.* **3**:569-581.

24. Schoettle, R.J., Kochanek, P.M., Magargee, M.J., Uhl, M.W., and Nemoto, E.M. (1990). Early Polymorphonuclear Leukocyte Accumulation Correlates with the Development of Posttraumatic Cerebral Edema in Rats. *J. Neurotraum.* **7**:207-217.

25. Keeling, K.L., Hicks, R.R., Mahesh, J., Billings, B.B., and Kotwal, G.J. (2000). Local neutrophil influx following lateral fluid-percussion brain injury in rats is associated with accumulation of complement activation fragment of the third component (C3) of the complement system. *J. Neuroimmunol.* **105**:20-30.

26. Mori, T., Wang, X., Jung, J., Sumii, T., Singhal, A.B., Fini, M.E., Dixon, C.E., Alessandrini, A., and Lo, E.H. (2002). Mitogen-Activated Protein Kinase Inhibition in Traumatic Brain Injury: *In Vitro* and *In Vivo* Effects. *J. Cerebr. Blood F. Met.* **22**:444-452.

27. Lum, H. and Roebuck, K.A. (2001). Oxidant stress and endothelial cell dysfunction. *Am. J. Physiol-Cell Ph.* **280**:C719-C741.

28. Gerritsen, M.E. and Bloor, C.M. (1993). Endothelial cell gene expression in response to injury. *Faseb J.* **7**:523-532.

29. Regan, R.F. and Choi, D.W. (1994). The effect of NMDA, AMPA/kainite, and calcium channel antagonists on traumatic cortical neuronal injury in culture. *Brain Res.* **633**: 236-242.

30. Shepard, S.R., Ghajar, J.B.G., Giannuzzi, R., Kupferman, S., and Hariri, R.J. (1991). Fluid percussion barotrauma chamber: A new *in vitro* model for traumatic brain injury. *J. Surg. Res.* **51**:417-424.

31. Topp, K.S., Faddis, B.T., and Vijayan, V.K. (1989). Trauma-Induced Proliferation of Astrocytes in the Brains of Young and Aged Rats. *Glia* **2**:201-2011.

32. Paemeleire, K. and Leybaert, L. (2000). ATP-Dependent Astrocyte-Endothelial Calcium Signaling Following Mechanical damage to a Single Astrocyte in Astrocyte-Endothelial Co-Cultures. *J. Neurotraum.* **17**:345-358.

33. Jayakumar, A.R., Rao, R., Panickar, K.S., Moriyama, M., Reddy, P.V.B., and Norenberg, M.D. (2008). Trauma-Induced Cell Swelling in Cultured Astrocytes. *J. Neuropath. Exp. Neur.* **67**:417-427.

34. Raghupathi, R. (2004). Cell Death Mechanisms Following Traumatic Brain Injury. *Brain Pathol.* **14**:215-222.

35. Rzalinski, B.A., Liang, S., McKinney, J.S., Willoughby, K.A., and Ellis, E.F. (1997). Effect of Ca^{2+} on In Vitro Astrocyte Injury. *J. Neurochem.* **68**:289-296.

36. Lamb, R.G., Harper, C.C., McKinney, J.S., Rzigalinski, B.A., Ellis, E.F. (1997). Alterations in Phosphatidylcholine Metabolism of Stretch-Injured Cultured Rat Astrocytes. *J. Neurochem.* **68**:1904-1910.

37. Neary, J.T., Kang, Y., Willoughby, K.A., and Ellis, E.F. (2003). Activation of Extracellular Signal-Regulated Kinase by Stretch-Induced Injury in Astrocytes Involves Extracellular ATP and P2 Purinergic Receptors. *J. Neurosci.* **23**:2348-2356.

38. Baeuerle, P.A. and Henkel, T. (1994). Function and Activation of NF-κB in the Immune System. *Annu. Rev. Immunol.* **12**:141-179.

39. Sasaki, C.Y., Barberi, T.J., Ghosh, P., and Longo, D.L. (2005). Phosphorylation of RelA/p65 on Serine 536 Defines an I κBα-independent NF-κB Pathway. *J. Biol. Chem.* **280**:34538-34547.

40. Mori, T., Wang, X., Aoki, T., and Lo, E.H. (2002). Downregulation of Matrix-Metalloproteinase-9 and Attenuation of Edema via Inhibition of ERK Mitogen Activated Protein Kinase in Traumatic Brain Injury. *J. Neurotraum.* **19**:1411-1419.

41. Kyriakis, J.M. and Avruch, J. (2012). Mammalian MAPK Signal Transduction Pathways Activated by Stress and Inflammation: a 10-Year Update. *Physiol. Rev.* **92**:689-737.

42. Dhandapani, K.M., Hadman, M., De Sevilla, L., Wade, M.F., Mahesh, V.B., and Brann, D.W. (2003). Astrocyte Protection of Neurons. Role of Transforming Growth Factor-β Signaling Via c-Jun-AP-1 Protective Pathway. *J. Biol. Chem.* **278**:43329-43339.

43. Zhu, D., Hu, C.H., Sheng, W., Tan, K.S., Haidekker, M.A., Sun, A.Y., Sun, G.Y., and Lee, J.C.M. (2009). NAD(P)H oxidase-mediated reactive oxygen species production alters astrocyte membrane molecular order via phospholipase A_2. *Biochem. J.* **421**:201-210.

44. Kramerov, A.A., Ahmed, K., and Ljubimov, A.V. (2012). Cell Rounding in Cultured Human Astrocytes and Vascular Endothelial Cells Upon Inhibition of CK2 is Mediated by Actomyosin Cytoskeleton Alterations. *J. Cell Biochem.* **113**:2948-2956.

45. Ramakers, G.J.A. and Moolenaar, W.H. (1998). Regulation of Astrocyte Morphology by RhoA and Lysophosphatidic Acid. *Exp. Cell Res.* **245**:252-262.

46. Cavalcanti-Adam, E.A., Volberg, T., Micoulet, A., Kessler, H., Geiger, B., and Spatz, J.P. (2007). Cell Spreading and Focal Adhesion Dynamics Are Regulated by Spacing of Integrin Ligands. *Biophys. J.* **92**:2964-2974.

47. Weksler, B.B., Subileau, E.A., Perrière, N., Charneau, P., Holloway, K., Leveque, Tricoire-Leignel, H., Nicotra, A., Bourdoulous, S., Turowski, P., Male, D.K., Roux, F., Greenwood, J., Romero, I.A., and Couraoud, P.O. (2005). Blood-brain barrier-specific properties of a human adult brain endothelial cell line. *Faseb J.* **19**:1872-1874.

48. Weksler, B., Romero, I.A., and Couraud, P. (2013). The hCMEC/D3 Cell Line as a Model of the Human Blood-brain Barrier. *Fluids Barrier CNS* **10**:16.

49. Zhu, D., Hu, C.H., Sheng, W., Tan, K.S., Haidekker, M.A., Sun, A.Y., Sun, G.Y., and Lee, J.C.M. (2009). NAD(P)H oxidase-mediated reactive oxygen species production alters astrocyte membrane molecular order via phospholipase A_2. *Biochem. J.* **421**:201-210.

50. Gadea, A., Schinelli, S., and Gallo, V. (2008). Endothelin-1 Regulates Astrocyte Proliferation and Reactive Gliosis Via a JNK/c-Jun Signalling Pathway. *J. Neurosci.* **28**:2394-2408.

51. Bennet, B.L., Sasakim D.T., Murray, B.W., O'Leary, E.C., Sakata, S.T., Xu, W., Leisten, J.C., Motiwala, A., Pierce, S., Satoh, Y., Bhagwat, S.S., Manning, A.M., and Anderson, D.W. (2001). SP600125, an anthrapyrazolone inhibitor of Jun N-terminal kinase. *P. Natl. Acad. Sci. USA* **98**:13681-13686.

52. Heo, Y., Kim, S., Seo, C.I., Kim, Y.K., Sung, B., Lee, H.S., Lee, J.I., Park, S., Kim, J.H., Hwang, K.Y., Hyun, Y., Jeon, Y.H., Ro, S., Cho, J.M., Lee, T.G., and Yang, C., (2004). Structural basis for the selective inhibition of JNK1 by the scaffolding protein JIP1 and SP600125. *EMBO J.* **23**:2185-2195.

53. De, S.K., Stebbins, J.L., Chen, L., Riel-Mehan, M., Machleidt, T., Dahl, R., Yuan, H., Emdadi, A., Barile, E., Chen, V., Murphy, R., and Pellecchia, M. (2009). Design, Synthesis, and Structure-Activity Relationship of Substrate Competitive, Selective, and *in Vivo* Active Triazole and Thiadiazole inhibitors of the c-Jun N-Terminal Kinase. *J. Med. Chem.* **52**:1943-1952.

54. McKinney, J.S., Willoughby, K.A., Liang, S., and Ellis, E.F. (1996). Stretch-Induced Injury of Cultured Neural, Glial, and Endothelial Cells: Effect of Polyethylene Glycol-Conjugate Superoxide Dismutase. *Stroke* **27**:934-940.

55. Chang, L., Jones, Y., Ellisman, M.H., Goldstein, L.S.B., and Karin, M. (2003). JNK1 is Required for Maintenance of Neural Microtubules and Controls Phosphorylation of Microtubule-Associated Proteins. *Dev. Cell* **4**:521-533.

56. Handa, O., Stephen, J., and Cepinskas, G. (2008). Role of endothelial nitric oxide synthase-derived nitric oxide in activation and dysfunction of cerebrovascular endothelial cells during early onset of sepsis. *Am. J. Physiol-Heart C.* **295**:1712-1719.

Curriculum Vitae

Name:	Claudia Augustine
Post-secondary Education and Degrees:	The University of Western Ontario London, Ontario, Canada Bachelor of Science, Honors Specialization in Biology *with Distinction,* Western Scholar 2007-2011
Honours and Awards:	Pediatric Graduate Student Stipend, Western University 2012, 2013 Quality of Life, Graduate Student Research Scholarship awarded by the Children's Health Foundation 2012 Graduate Thesis Research Award 2013
Abstract Acceptance/ Academic Meetings Attended:	Experimental Biology 2013 (Boston, MA, USA) Poster Presenter Critical Care Canada Forum 2012 (Toronto, Canada) Poster Presenter Infection and Immunity Research Forum 2012 at Western University (London, Canada) Poster Presenter Physiology and Pharmacology Research Day 2012 at Western University (London, Canada) Poster Presenter Pediatrics Research Day 2012 at Western University (London, Canada) Oral Platform Presenter London Health Research Day 2012 (London, Canada) Poster Presenter